Final Appendix CI

Hydrology

Rahway River Basin, New Jersey
Flood Risk Management Findings Report

September 2025

**New Jersey Department of
Environmental Protection**

**U.S. Army Corps of Engineers
New York District**

LIST OF TABLES

LIST OF FIGURES

1.0 INTRODUCTION

1.1 Area of Study

The Rahway River Basin is located in northeastern New Jersey. It lies within the metropolitan area of New York City. The basin is approximately 83.3 square miles (53,300 acres) in area. A feasibility study was conducted in September 2016 for the "fluvial," or inland portion of the basin. Another feasibility study was conducted in January 2020 for the coastal portion of the basin and includes the New Jersey municipalities of Rahway, Carteret, and Linden. This Findings Report focuses on the entirety of the Rahway River Basin. A map of the Rahway River Basin, its municipalities, and the fluvial and coastal study areas is shown in Figure 1.
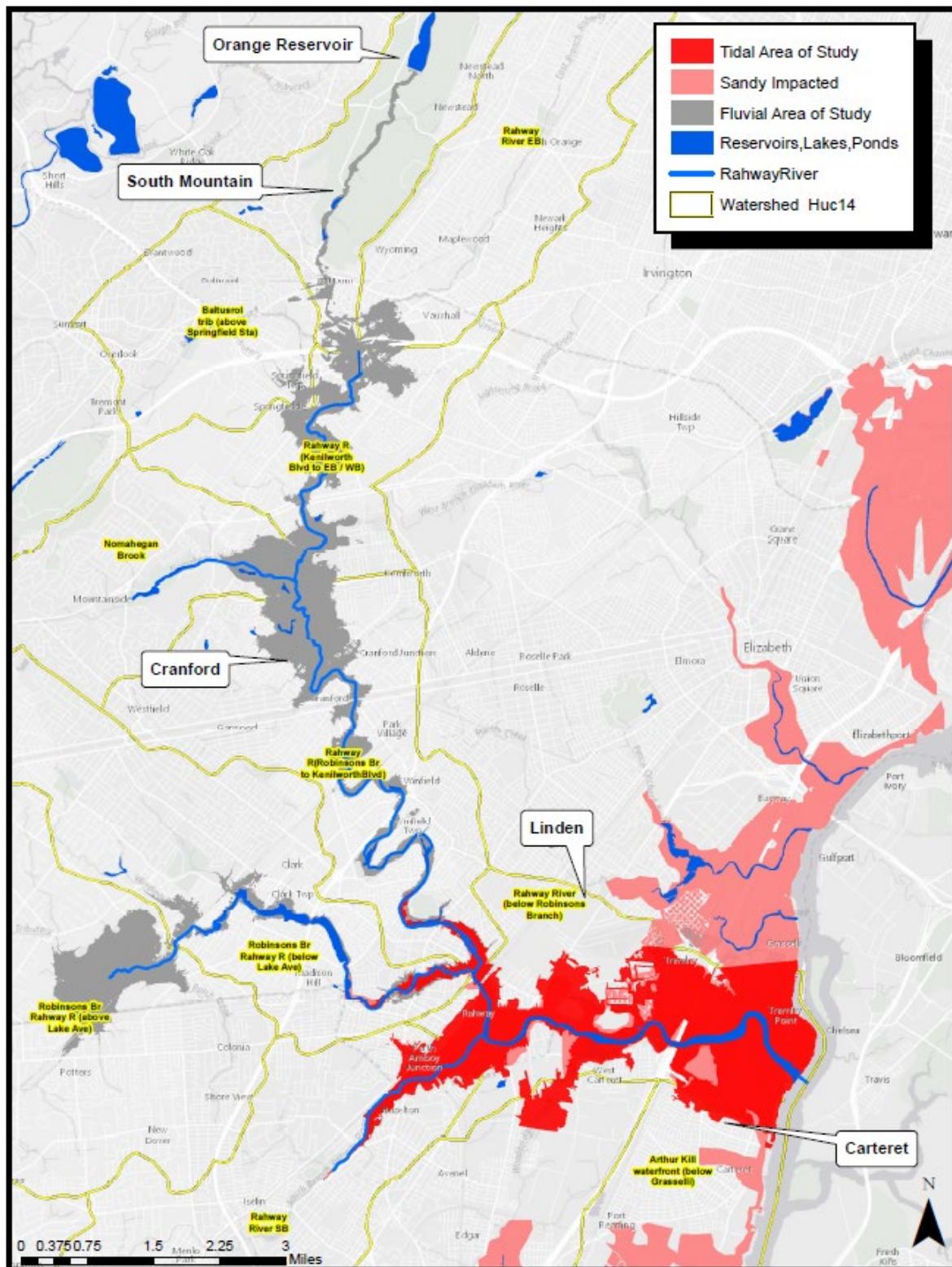
Figure 1: Rahway River Watershed

1.2 Present Flooding Problems

Periodic storms have caused severe fluvial flooding along the Rahway River. There are several main areas with high flood risk: the Townships of Millburn and Cranford and the Robinsons Branch in Rahway. Flooding in Millburn is caused by low channel capacity and the presence of several restricted bridges on the Rahway River. Flooding along the Rahway River in Cranford is caused by low channel capacity, constrictions of several bridges and dams along the river and two 90-degree bends forming a "U" turn at Springfield Ave. just upstream of the center of the Township. The flood waters back up from the main Cranford area into the area of Lenape Park Detention Basin and Kenilworth Township. In the City of Rahway at Robinson's Branch the high risk of flooding is due to low channel capacity, the constrictions of several bridges, and the compound tidal/fluvial backwater from the main stem of the Rahway River, which is independent of the hydraulic conditions in the Robinson's Branch.

Flooding problems are also identified in minor tributaries of Rahway River. Gallows Hill Brook experiences significant flooding due to local issues such as sediment buildup, which reduces channel capacity, and minimal maintenance since its 1981 flood control project. The rectangular channel, which is 10-feet-wide and has 5.5-foot-high walls, faces overtopping risks during short, high-intensity storms in its 1.2-square-mile drainage area. Flooding is primarily driven by local conditions and limited culvert capacity, rather than backwater from the Rahway River.

1.3 Objective

The objective of this study is to identify a feasible means of managing the risk of flooding in the most affected areas of the Rahway River in the most cost-effective manner in an environmentally and culturally acceptable way. The flood risk management concepts considered in this study are: channel modification, bridge replacement, dams, levees, pump stations, and nonstructural measures. Authorized improvements to tidal gates are currently under design and not considered in this study.

1.4 Scope of Work

This Findings Report encompasses a range of activities, including updating models, analyzing stage frequency curves, conducting detailed analyses, and developing conceptual plans.

Existing hydrologic (HEC-HMS) and hydraulic (HEC-RAS) models were provided by the USACE. An additional reach was incorporated into the model to represent the East Branch of the river, and publicly available data (e.g., LIDAR and FEMA data) was utilized to estimate stream bed cross-sections and adjacent land data. These cross-sections were georeferenced to be used in the model.

The models were updated with the latest hydrologic and hydraulic data available and calibrated to Hurricane Irene and Tropical Storm Ida. The boundary conditions for the downstream end of the model determined in the Tidal Feasibility Study were used in this study. The models were calibrated to multiple points within the specified peak events (Irene and Ida).

The existing conditions of the floodplain were analyzed to confirm that they are reflective of the observed conditions. The model was calibrated to publicly available floodmarks and stream gage data. A HEC-RAS model was developed and calibrated to produce stage-frequency data and profiles for existing conditions. The updated hydrology model (HEC-HMS) was calibrated to the full Rahway River Basin, including the tidally influenced areas. The analysis of the boundary between tidal/storm surge dominated areas and the fluvial dominated flood areas was evaluated using a compound flooding assessment. Statistical analysis was conducted to cover the full-range probabilities of all possible coincidental combinations.

2.0 RAHWAY RIVER DESCRIPTION

2.1 General

The Rahway River Basin is located in northeastern New Jersey. It lies within the metropolitan area of New York City and occupies portions of Essex, Union and Middlesex Counties. The entire watershed is approximately 83.3 square miles in area and is roughly crescent or "L"-shaped. Its greatest width is approximately 10 miles in the east-west direction, from the City of Linden to the City of Plainfield. Its greatest length is approximately 18 miles in a north–south direction, from West Orange to Metuchen. The Raritan River, from the East and West Branch Confluence to it mouth (confluence with Arthur Kill) is approximately 19 miles. The major tributaries to the Rahway River are the following: East and West Branch of the Rahway River, Robinsons Branch and South Branch of the Rahway River. The major towns and communities that are within this watershed are the following: Essex County (e.g. Orange, Milburn), Union County (e.g. Springfield, Kenilworth, Cranford, Clark, Linden, and Rahway). A map of the Rahway River basin and the municipalities that make it up is shown on Figure 2.

The Rahway River is underlain by Triassic age fractured red shales and sandstones of the Brunswick formation. The entire study area is overlain by unconsolidated material deposited during the Wisconsin glacial epoch. Thickness ranges from 0 to over 70 feet with an average depth of 30 feet. The majority of the study area is underlain by boulders. The areas immediately upstream of the Robinson's Branch-Rahway River junction and downstream of the US Route 22 Bridge are overlain by stratified drift. These flat lying deposits consist of well-sorted bands of clay, silt, sand and gravel. In the Springfield-Union area, the Rahway River cuts through rolling topography of a recession moraine. The moraine material ranges from clay to boulders and is mostly unstratified except for some local bedding. Each of these glacial deposits are overlain by thin postglacial deposits of silty loan. Section 7.0: HYDROLOGIC MODEL goes into greater detail about the watershed and physical parameter development for the Rahway River Basin.
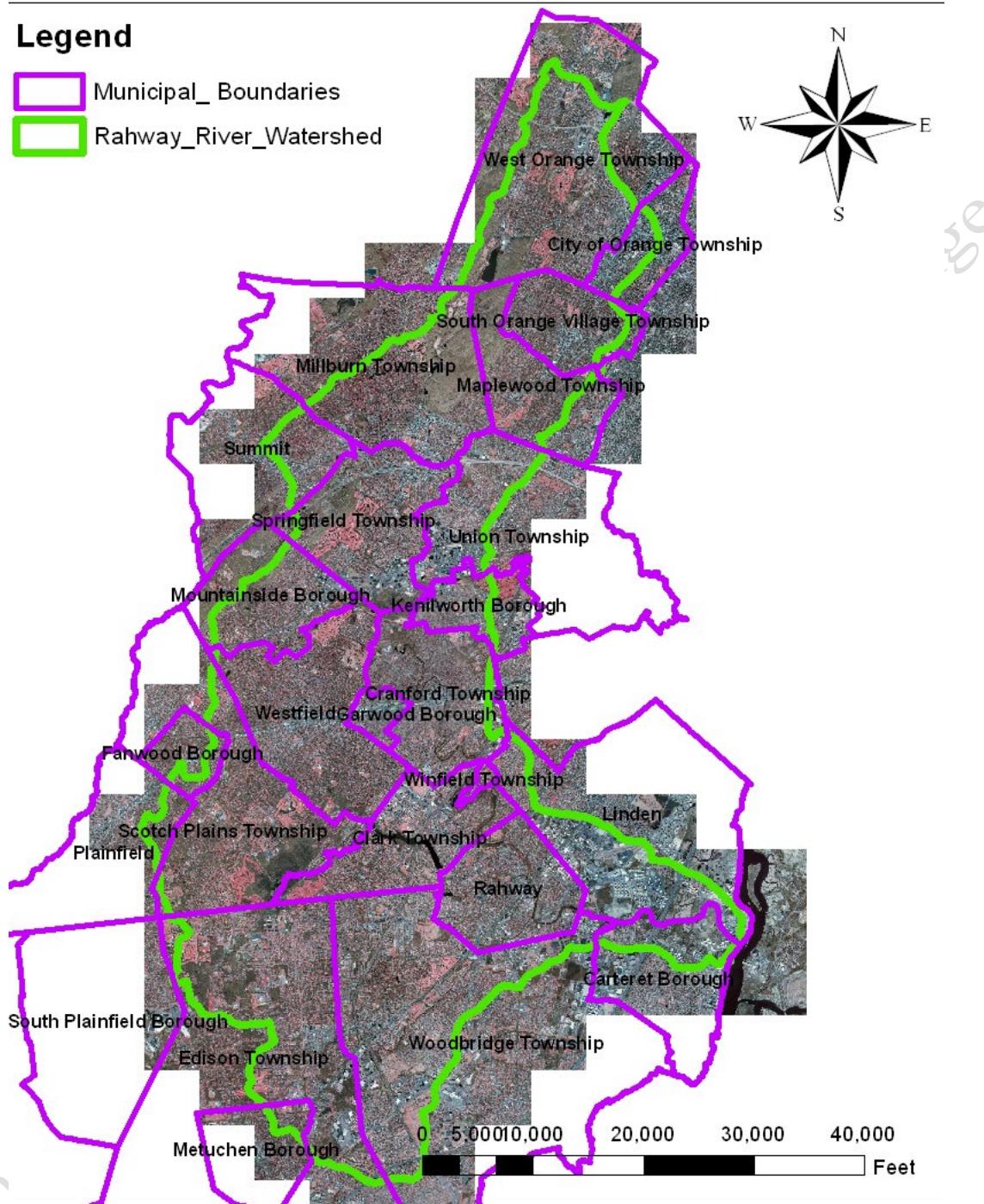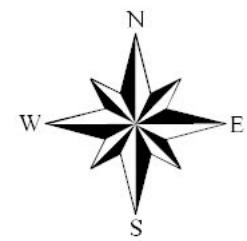
Figure 2: Rahway River Basin with Corresponding Municipalities

2.2 Flood Prone Areas

The Rahway River in the Townships of Millburn and Cranford and Robinson's Branch at Rahway begin to experience major fluvial flooding at and above the 10% chance of annual exceedance (10-yr) event.

At this stage, the areas upstream of Essex St and Oakland Rd experience flooding due to low channel capacity and the presence of restricted bridges on the Rahway River. The low-lying area between Park Dr. and Springfield Ave. near the Nomahegan Park Back experiences flooding due to back water from a tributary of the Rahway River and some street flooding upstream of Hansel Dam. For peak flows between the 10% chance of annual exceedance (10-yr) and the 4% chance of annual exceedance (25-yr) events, water surface elevations (WSEs) in the Rahway River overtop the Nomahegan Park levees. Although there are some inconsistencies in the top elevation of the levees, both sides of the levee system can contain approximately the same event. For storm events above the 4% chance of annual exceedance (25-yr), the stage of the Rahway River waters starts producing floods in the following areas:

1. Kenilworth residential area due to backwater caused by the constrictions of the Kenilworth Blvd. Bridge.

2. At the right overbank between Willow St. and Brookside Place, near Cranford High School.

3. On the left and right sides overbanks and behind the existing levee system, the residential area at the residential area surrounding Riverside Dr., Brookdale Rd., Edgewood Rd., Glenwood Rd., Summit Rd., Edgar Ave., Franklin Ave., Balmiere Pkwy. and Doering Way.

4. And the commercial area surrounding Chestnut St.

3.0 PROJECT AREA

The Rahway project area is located along East Branch, West Branch, the Rahway River main steam, and Robinsons Branch. Fluvial flood damages occurred within the Townships of Millburn and Cranford and City of Rahway from Tropical Storm Floyd (September 1999), April 2007 Nor'easter, Tropical Cyclone Irene (August 2011), and Tropical Cyclone Ida (August 2021). Also, coastal damages occurred within the City of Rahway from Tropical Cyclone Sandy.

4.0 CLIMATOLOGY

4.1 Climate

The climate of the Rahway River basin is characteristic of the entire Middle Atlantic Seaboard. Marked changes of weather are frequent, particularly during the spring and fall. The winters are moderate in both temperature and snowfall. The summers are moderate, with hot sultry weather in mid-summer, and with frequent thunderstorms. Rainfall is moderate, and well-distributed throughout the year. The relative humidity is high.

4.2 Precipitation Stations and Data

Stations that were used for historic precipitation records in this study include:

Rainfall Station Canoe Brook (ID 281355); Lat/Long: 40º 45'N74º02'W; Elev: 180 feet

Rainfall Station: Newark Airport (ID 286026); Lat/Long: 40º 41'N74º10'W; Elev: 7 feet

Rainfall Station: Cranford (ID 282023); Lat/Long: 40º 39'N74º18'W; Elev: 75 feet

Rainfall Station: Plainfield (ID 287079); Lat/Long: 40º 36'N74º24'W; Elev: 90 feet

Furthermore, to enhance accuracy, 4km-grid radar data were obtained from the National Weather Service (NWS) of NOAA. The extracted data are from Analysis of Record for Calibration (AORC) section of their website for the North-East region. The recorded data from these stations were used to develop selected historic storm events within the Rahway River Basin and is explained in detail in the following paragraphs.

Two historic events were selected for calibration analysis for this watershed. The storms that were chosen are the August 27-28 event in 2011, also known as Tropical Storm Irene, and the September 1 event in 2021, known as Tropical Storm Ida. Precipitation data for Hurricane Irene covers the timeline of 08/27/2011 to 08/31/2011, while data for Hurricane Ida spans from 08/31/2021 to 09/05/2021. The resolution of the precipitation data was 4km x 4km, and the radar datasets were then cropped into the area of interest to reduce computation loading. Since the grid set precipitation was recorded in the UTC time zone on the NOAA website, the data was shifted by 4 hours to align with the Eastern Time zone.

4.3 Annual (Daily) and Monthly Precipitation

The mean annual precipitation in the Rahway River Watershed is approximately 50.94 inches from the 1971-2000 based on monthly normals for the Cranford, New Jersey Station. The observed highest daily value at this station was 9.76 inches (Tropical Storm Floyd). The monthly extremes were 13.96 inches in July 1975 and 0.45 inches in November 1976. The distribution of precipitation throughout the years is fairly uniform with the highest amount occurring during the summer months. The mean annual snowfall is 20.00 inches at Cranford, New Jersey precipitation station.

4.4 Storm Types

The storms which occur over the northeastern states have their origins in or near the Pacific and the North Atlantic oceans and may be classified as: extratropical storms; which include thunderstorms, nor'easters, and cyclonic storms; or tropical storms which include hurricanes. The thunderstorms, due to rapid convective circulation, usually occur in spring or summer and are limited in extent and typically cause local flooding on "flashy streams". Extra-tropical/Cyclonic storms, due to their transcontinental air mass movement with attendant "highs" and "lows," usually occur in the winter or early spring and is a potential flood-producer over large areas because of its widespread extent. Hurricanes and tropical storms proceed northward along the coastal areas, are accompanied by strong winds and torrential rains. Rainfall is enhanced when a tropical marine air mass is lifted suddenly on contact with hills and mountainous terrain, causing heavy rains usually in the summer and fall seasons.

4.5 Past Storms/Historical Floods

A review of storms which have occurred in the northeastern states reveals that the Rahway River basin is located in the center of the North Atlantic storm belt. The interested reader can find brief descriptions of the following major flood- producing storms in the Rahway River basin presented in the *General Design Memorandum, Robinson's Branch of the Rahway River at Rahway, New Jersey Flood Control Study*, Volume 2, dated February 1986: (November 1977, July 1975, August 1973, August 1971, August 1969, May 1968 and July 1938). There were four large storms that effected the area of study with devastating flooding but only the two more recent ones (Irene and

Ida) were used to calibrate the HEC-HMS hydrologic model of the Rahway River basin. Detailed descriptions of these events are included in the storm descriptions below.

4.5.1 Tropical Storm Floyd

The eye of Floyd made landfall on 16 September 1999 near Cape Fear, North Carolina with Category 2 winds of 105 mph. After crossing eastern North Carolina and Virginia, Floyd weakened to a tropical storm. Its center then moved offshore along the coasts of the Delmarva Peninsula and New Jersey. On 17 September, the center of Floyd moved over Long Island NY (making landfall again roughly at the Queens-Nassau counties border) and New England, where it became extratropical.

Precipitation from the storm preceded its center in the New York City area on 15 September. Rainfall totals from Floyd were as high as 12 to 16 inches over portions of New Jersey, 4 to 8 inches over southeastern New York, and up to 11 inches over portions of New England. The inland flooding from Floyd was a disaster of immense proportions in the Eastern United States, particularly in North Carolina. The 56 direct deaths in the USA due to Floyd was the largest hurricane death toll since Agnes caused the deaths of 122 people in 1972. Total USA damage estimates range from three to over six billion dollars.

Floyd resulted in new flood peaks of record at sixty or more stream gages within the portions of New Jersey and New York contained by the New York District's civil works boundaries. Within the Rahway River basin, the total rainfall at Cranford, NJ was 10.82 inches. Tropical Storm Floyd produced a peak flow at the Springfield (USGS Gage 1394500) of 7990 cfs and a peak flow of 5590 cfs at the Rahway (USGS Gage 1395000).

4.5.2 April 15-16 2007 Nor'easter

The 15-16 April 2007 nor'easter dropped about three to ten inches of rain on the watersheds within the New York District's civil works boundaries between the early morning of Sunday 15 April 2007 and the early afternoon of Monday 16 April 2007, resulting in new flood peaks of record at ten USGS gages in New Jersey. This storm had the greatest flooding impact on the Raritan and Passaic River basins. It produced the worst flooding in the Raritan River basin since Tropical Storm Floyd during September 1999. Bound Brook and Manville were once again hit hard, as were

communities on the other side of the Raritan River in Middlesex County. Lincoln Park in the Passaic Basin was also hit hard.

The approximate time distribution of the total rainfall of the 15-16 April 2007 nor'easter over the watersheds of the New York District was an average of 7 to 7 ½ inches between about 2 a.m. on Sunday 15 April to 2 p.m. on Monday 16 April 2007, with most within the 24 hours beginning at 2 a.m. on Sunday 15 April. The greatest hourly amounts were from 0.6 to 0.8 inches at about 2 p.m. on Sunday 15 April 2007.

Unlike Tropical Storm Floyd, which broke the summer 1999 drought and fell on dry ground, the April 2007 nor'easter caused as much flooding as it did because it was preceded by the smaller 1-2 March and 12-13 April 2007 storms and fell on saturated ground.

The Nor'easter had a drop in central pressure of 0.83 inches in 24 hours, which qualified it as a meteorological bomb (a drop in central pressure of at least 0.71 inches in 24 hours). The lowest central pressure of about 28.53 inches is near the border of the pressure defined Categories 2 and 3 once used on the Saffir-Simpson Hurricane Scale.

Within the Rahway River basin, the total rainfall at Cranford was 6.47 inches. This nor'easter produced a peak flow at the Springfield USGS gage of 5540 cfs and a peak flow of 4910 cfs at the Rahway USGS gage.

4.5.3 Tropical Cyclone Irene

Tropical cyclone Irene began as a tropical wave off the West African coast on 15 August 2011. The storm was upgraded into Tropical Storm Irene at 23:00 UTC on 20 August about 190 miles east of Dominica in the Lesser Antilles. On 22 August Irene made landfall near Punta Santiago, Humacao, Puerto Rico, with estimated sustained winds of 70 mph. Just after its initial landfall, Irene was upgraded to a Category 1 hurricane, the first of the 2011 Atlantic hurricane season.

Moving erratically through the southeast Bahamas over very warm waters, Irene quickly expanded as its outflow aloft became very well established. The cyclone intensified into a Category 3 hurricane. Early on 27 August, Irene weakened to a Category 1 hurricane as it approached the Outer Banks of North Carolina. At 7:30 am EDT the same day, Irene made landfall near Cape Lookout, on North Carolina's Outer Banks, with winds of 85 mph. Later on 27 August, Irene re-

emerged into the Atlantic near the southern end of the Chesapeake Bay in Virginia. At about 09:35 UTC on 28 August, Irene made a second landfall at the Little Egg Inlet on the New Jersey shore with winds of 75 mph, and soon after moved over water again. Hours later, Irene weakened to a tropical storm with winds of 65 mph near New York City. Irene then moved northeast over New England, becoming post-tropical over the state of Maine at 11:00 pm EDT.

Significant damage occurred in North and Central New Jersey, where flooding was widespread. Severe river flooding took place on the Raritan, Millstone, Rockaway, Rahway, Delaware, and Passaic Rivers due to record rainfall. The highest rainfall recorded in the state was in Freehold (11.27 inches), followed by Jefferson (10.54 inches) and Wayne (10.00 inches). The flooding affected roads, including the heavily used Interstate 287 in Boonton, where the northbound shoulder collapsed, the Garden State Parkway, which flooded in Cranford from the Rahway River and in Toms River near exit 98. Along the Hudson River, in parts of Jersey City and Hoboken, flood waters rose as much as 5 feet and the north tube of the Holland Tunnel was briefly closed. In total, ten deaths within the state are attributable to the storm.

In addition to major flooding, the combination of already heavily saturated ground from a wet summer and heavy wind gusts made trees in Union County especially vulnerable to wind damage. Fallen trees, many pushed from the soaked ground with their roots attached, blocked vital roads from being accessed by local emergency services. Numerous homes suffered structural damage from the winds, and limbs impacting their roofs. Around Union County, fallen wires in combination with flooded electrical substations left parts of Union County, including Cranford, Garwood, and Westfield without power or phone service for nearly a week. In total, approximately 1.46 million customers of Jersey Central Power and Light (JCP&L) and Public Service Electric and Gas (PSEG) lost power throughout most of the 21 counties.

On 29 August, the governor of New Jersey asked President Obama to expedite release of emergency funds to the state. Eventually all 21 New Jersey counties became eligible for FEMA aid.

4.5.4 Tropical Cyclone Sandy

Sandy was a classic late-season hurricane in the southwestern Caribbean Sea but weakened into a tropical storm north of the Bahamas Islands. The system re-strengthened into a hurricane while it

moved northeastward, parallel to the coast of the southeastern United States, and reached a secondary peak intensity of 85 knots while it turned northwestward toward the Mid-Atlantic States. Sandy weakened somewhat and then made landfall as a post-tropical cyclone near Brigantine, New Jersey. Sandy was predominately a coastal storm and not much of a rainfall producer in the project area and did not provide any impact from runoff. Only 1.33 inches of precipitation was recorded at Newark Airport on 29-30 October 2012.

4.5.5 Hurricane Ida

Hurricane Ida, originating as a tropical depression in the Caribbean Sea on August 26, 2021, rapidly intensified into a Category 4 hurricane, making landfall in Louisiana on August 29 with sustained winds of 150 mph. As it moved inland, Ida weakened but maintained significant strength, traveling northeastward and bringing catastrophic rainfall and flooding to the Northeastern United States. By September 1, remnants of Ida interacted with a stationary front in the mid-Atlantic, producing a historic rainfall event across the region, including New Jersey and the Rahway River basin.

In New Jersey, Hurricane Ida set new rainfall records in many areas. For instance, Newark experienced its wettest day on record, with over 8 inches of rainfall. The flooding from Ida in New Jersey was catastrophic. Several rivers, including the Rahway River, surged beyond their banks, inundating homes, businesses, and infrastructure. Streets turned into rivers, and vehicles were swept away in the torrent. Cranford, Garwood, Westfield, and Rahway were among the hardest-hit towns within the Rahway River basin, with extensive damage reported to residential neighborhoods and public utilities.

The rainfall intensity of Hurricane Ida overwhelmed the state's stormwater infrastructure. In some areas, rain rates exceeded 3 inches per hour, leading to flash flooding conditions. The unprecedented inundation prompted swift water rescues, and thousands of residents were evacuated. Union County alone reported significant losses, including damage to bridges, culverts, and electrical substations.

In addition to flood damage, Hurricane Ida caused widespread power outages. Approximately 1.2 million customers in New Jersey experienced service interruptions, with some outages lasting several days. Roads remained impassable for extended periods due to floodwater and debris.

Hurricane Ida resulted in at least 30 fatalities in New Jersey, the highest death toll of any state impacted by the storm. Most of the deaths were attributed to flash flooding, particularly in urban and suburban areas where swift-moving water trapped individuals in vehicles and basements.

Following the storm, the President issued a major disaster declaration, making all 21 New Jersey counties eligible for FEMA assistance.

4.6 Climate Change

Hydrologic and coastal processes have the potential to be sensitive to climate change and thereby have the potential to affect the performance of the coastal storm risk management features proposed in the Rahway River Basin. Consistent with the objective of ECB 2018-14 (Guidance for Incorporating Climate Change Impacts to Inland Hydrology in Civil Works Studies, Designs, and Projects), to enhance the climate preparedness and resilience of USACE projects by incorporating relevant information about observed and expected climate change impacts in hydrologic analysis for planned, new, and existing USACE projects, a qualitative analysis for inland hydrology was conducted using the best available data for the Rahway River basin. The quantitative analysis was conducted in three phases as specified by ECB 2018-14: Initial Scoping, Vulnerability Assessment, and a Risk Assessment.

4.6.1 Phase I Initial Scoping

The Rahway River Basin is subjected to both precipitation and coastal storm events and has experienced severe flooding during to coastal storm surge events. Due to the project area being affected by both inland hydrology and coastal storms, this analysis will focus on observed and projected trends in precipitation, streamflow, and sea level rise (SLR).

This appendix will focus on a qualitative analysis of hydrology by performing a vulnerability assessment by performing a review of available literature sources and using the tools developed by USACE including the Climate Vulnerability Assessment Tool, The Climate and Hydrology Assessment Tool (CHAT), and the non-stationarity detection tool. Since SLR directly impacts the tailwater conditions in the hydraulic model, the assessment for sea-level rise can be found in the Hydraulics Appendix CII.

4.6.2 Phase II Vulnerabiity Assessment

For the vulnerability assessment phase, information was collected and analyzed to determine whether changes are presently occurring and whether expected changes in future hydrologic conditions will result in performance requirements significantly different from the present.

The vulnerability assessment includes a literature review of current climate and observed and projected climate trends and application of climate tools used to provide information on observed and projected climate trends relevant to the project area.

4.6.2.1 Literature Review

A synthesis of the USACE peer-reviewed climate literature is available for the Mid-Atlantic Region and was one of the primary sources of information referenced in this literature review. Additionally the Fourth National Climate Assessment produced by the US Global Change Research Program was used as a source for understanding observed and projected climate trends in the northeast. The USACE report summarizes observed and projected climate and hydrological patterns cited in reputable peer-reviewed literature and authoritative national and regional reports, and characterizes climate threats to the USACE business lines (USACE, 2015a). The project watershed falls within the Mid-Atlantic Region, which is also referred to as Water Resources Region 02 (2-digit hydrologic unit code, or HUC02); see Figure 23.

4.6.2.2 Observed Climate Trends

Based on the observations made by the Fourth National Climate Assessment for the Northeast region, river flooding will pose a growing challenge to the Northeast region's systems and infrastructure will be increasingly compromised by future intense precipitation events. The Northeast has experienced a greater recent increase in extreme precipitation than any other region in the United States; between 1958 and 2010, the Northeast saw more than a 70 percent increase in the amount of precipitation falling in very heavy events (defined as the heaviest 1 percent of all daily events). Winter and spring precipitation is projected to increase; winter precipitation by about 5 to 20 percent by the end of the century.

In the Climate Change and Hydrology Literature Synthesis for the US Army Corps of Engineers Missions in the United States for the Mid-Atlantic Region 2, the USACE Institute of Water Resources cites Burns et al. (2007) identified statistically significant ($p<0.05$) increasing trends in

annual precipitation for half of their climate stations in the Catskill Mountains in Southern New York. These authors used data from the period 1952-2005, and quantified average rates of increase in annual precipitation in the range of 79-263 mm per fifty years of record. However, no such trend was found by Warrach et al. (2006) for a climate station also in southern New York State. These authors analyzed annual precipitation totals for the period 1900-2000. While no significant annual trends were detected, seasonal trends were detected: including decreasing winter and summer monthly precipitation totals. The overall summary of observed climate trends indicates "there is also a good consensus in the literature that precipitation, and the occurrence of extreme storm events, has increased over the past century in the study region. However, despite the increased precipitation in the region, there is no evidence of significant increases in streamflow over the same period".

The conclusion may suggest that increased evaporation due to changing temperatures, changes in land usage, and channel diversion changes, or other factors may offset the increased amount of precipitation showing up in the form of increase streamflow. Projected climate trends in this report indicate "the majority of the studies reviewed here project increases in precipitation and streamflow through the 21st century. Extreme high events (storms and floods), in particular, are projected to increase in the future. Low flows, however, have been projected to decrease in the future as a result of the projected temperature (and ET) increases." A summary of the observed and projected climate variables is shown in Figure 24.

4.6.2.3 Projected Climate Trends

In the Climate Change and Hydrology Literature Synthesis for the US Army Corps of Engineers Missions in the United States for the Mid-Atlantic Region 2, the USACE Institute of Water Resources cites Najjar et al. (2009). This data quantifies an ensemble mean increase in annual precipitation for three major Mid-Atlantic watersheds. Mid and end of century projections show an average 2-5% increase in annual precipitation for the study region compared to the historical baseline (1971-2000). However, the uncertainty in these projections is reflected with relatively high standard deviations (3-12%) associated with these values.

Future projections of extreme events, including storm events and droughts forecasts increases in the occurrence and intensity of storm events by the end of the 21st century for the general study

region. Wang and Zhang (2008) used downscaled GCMs to look at potential future changes in precipitation events across North America. They used an ensemble of GCMs and a single high emissions scenario (A2) to quantify a significant increase (20-50%) in the recurrence of the current 20-year 24-hour storm event for their future planning horizon (2075) and the General Mid-Atlantic Region. Additional uncertainty is introduced by the use of hydrologic models, there is moderate consensus that flows, particularly peak flows, will increase in the region through the 21st century as a result of increased precipitation. Low flows, however, are generally projected to decrease in the future. However, the frequency of heavy downpours is projected to continue to increase as the century progresses. Figure 25 summarizes the projected climate trends and impacts on each of the USACE business lines.

4.6.2.4 Climate Hydrology Assessment Tool

The Climate Hydrology Assessment Tool (CHAT) assess trends in both observed and projected hydrometeorological data to project future changes in streamflow using GCMs at the watershed scale (HUC 04) seen on Figure 26. The USGS maintains two gages on the Rahway River: 01395000 Rahway River at Rahway, NJ and 01394500 Rahway River near Springfield, NJ. Annual peak instantaneous flow data was available from 1922 to 2013 for the Rahway River at Rahway (01395000), and from 1938 to 2013 for the Rahway River near Springfield (01394500) in the CHAT tool for analysis, and were used for the basis of this analysis. No information was available for the Robinsons Branch at Rahway (01396000) from the CHAT tool.

Observed Trends

A liner regression analysis performed by the CHAT tool indicates an upward trend in annual peak discharges for both gages. The p-value associated with the trendline at the Rahway gage at Rahway, NJ is less than 0.0001 and is 0.001416 for the Rahway River gage near Springfield as shown in Figures 27 and 28 respectively. Both p-values are considered statistically significant. A p-value of 0.05 or less is typically used a threshold for statistical significance in this analysis. These results indicate there may an increasing trend in peak flow in the basin.

Projected Trends

The CHAT displayed a range of projected, unregulated, annual maximum monthly streamflow computed by 93 different combinations of GCM outputs. Climate changed hydrology is generated

for a period from 1952-2099 in the HUC 0203 of Lower Hudson-Long Island as shown in Figure 29.

A statistical analysis of the projected hydrology from 1952-2099 indicates a statistically significant linear trend (p-value less than 0.0001) of increasing average annual monthly stream flows as shown in Figure 30. This data indicates there is a potential for increases in streamflow, which his consistent with the findings in the literature review.

4.6.2.5 Vulnerability Assessment Tool

The USACE Vulnerability Assessment tool is necessary to help guide adaptation planning and implementation so that USACE can successfully perform its missions, operations, programs, and projects in an increasingly dynamic physical, socioeconomic, and political environment. This tool provides indicators to develop vulnerability scores specific to each of the watersheds located within the contiguous United States.

A Vulnerability Assessment was conducted in the USACE North Atlantic Division (NAD), and within the New York District (NAN). Table 15 lists the vulnerability scores for the Flood Risk Reduction Business Line for HUC 0203, as well as the ranges of scores nationally, and within NAD and NAN for scenario changes in Table 15. As shown in the table, this watershed vulnerability of the Flood Risk Reduction business line is ranked the highest within the ranges NAN and NAD for all scenarios (wet and dry). When comparing these scores nationally, the HUC 0203 watershed falls within the middle for dry scenarios and below average for wet scenarios. Further analysis using the VA tool characterizes the HUC 0203 watershed as vulnerable for all scenarios for the Flood Risk Reduction Business Line when compared to the rest of the nation (top 20%).

The VA tool analyzed changes that were centered on two epochs, 2050 (2035-2065) and 2085 (2070-2099) grouping those epochs in "wet" and "dry" scenarios. Projections with total runoff values above the median value for the set are grouped as "wet", and ones with total runoff values below the median are grouped as "dry". All results were then given in scenario-epochs; Dry-2050, Dry-2085, Wet-2050, and Wet-2085. Several indicators localized within NAN were used to determine the overall climate risk score. These indicators include: Acres of Urban Area within 500-Year Floodplain (590), Flood Magnification Factor (568C/568L), and Percent Change in

Runoff divided by Percent Change in Precipitation (277), and Annual Coefficient of Variant (CV) of Unregulated Runoff (175C).

The indicator that dominates vulnerability in both scenarios is Indicator #568C (flood magnification factor) which contributes approximately 41% for both dry epochs, and 43% for both wet epochs with indicator values greater than 1 (1.124 and 1.14 for Dry-2050 and Dry-2085 respectively; and 1.2311 and 1.3381 for Wet-2050 and Wet-2085 respectively) which indicates positive increases in future flood flows for both dry and wet scenarios. Meanwhile, Indicator #590 (area of the 500-year flood plain) has the second highest contribution with roughly 26% for both dry and wet epochs which suggests higher vulnerability relative to other watersheds. The use of this tool suggests that "dry" scenario-epochs are vulnerable and considerations should be given to projects located within the urbanized 500-year flood plain area. Table 16 provides absolute values of all relative indicators for both scenarios and epochs indicating the percent contribution to the overall vulnerability score.

The results of the VA tool analysis indicate that the HUC 0203 watershed is vulnerable to impacts to the Flood Risk Reduction Business Line and should be taken in consideration during the planning process and in communication with the local sponsor.

4.6.2.6 Nonstationarity Detention Tool

Nonstationarity Detection Tool

The nonstationarity detection tool (NDT) was utilized for both the Rahway River at Rahway and the Rahway River near Springfield gages. The NDT detected a strong nonstationarity in annual peak streamflow in the year 1965 (3 distribution and 2 mean) for both gages as shown in Figures 31 and 32. A nonstationarity is considered strong when there is consensus among a minimum of three NDT detection methods, robustness in detection of changes in statistical properties, and relatively large change in the magnitude of a dataset's statistical properties (mean or standard deviation).

Monotonic Trend Analysis

A monotonic trend analysis is conducted to identify statistically significant trends in peak streamflow. Since strong nonstationarities were detected in both gage records, a monotonic trend

analysis was performed for both gage records starting in the year 1965. As shown in Figure 33 and 34, no monotonic trends were detected for either gage records.

Based on this criteria, the water year of 1965 is considered a strong change point due to an influx in urbanization with changes in streamflow, and changes in land use denoting the construction of the Lenape Flood Control Dam, gate operations at Hansels Dam and Taylor Park Dam, and the diversion of municipal water supplies (https://waterdata.usgs.gov/nwis/uv?site_no=01395000) which should be considered in hydrologic analysis. One method for doing so may be to perform a flood-frequency analysis using the period of record post 1965 while consider those aforementioned factors into account.

4.6.3 Phase III Risk Assessment

The Phase II vulnerability assessment conducted on the Lower Hudson – Long Island basin indicates that the project area is located in a 2-digit HUC watershed that is vulnerable to the effects of climate change. The HUC 0203 watershed is vulnerable to impacts from the Flood Risk Reduction Business Line. The best available scientific evidence based on climate literature and the Vulnerability Assessment tool indicates projected moderate increases precipitation and peak streamflow, as well as increases in storm frequency and intensity in the future. However, due to lack of quantitative hydrologic information, the impact of climate change to the project hydrology is inconclusive. Increases and storm frequency and intensity in the future may lead to increases in stream flow and instances of elevated river stages in the Rahway River, which may lead to more frequent overtopping instances of the levee feature in the future. However, due to the proximity of the basin to the Atlantic coastline the Rahway River is also influenced by sea level rise as documented in the Hydraulics Appendix. The proposed flood risk reduction features (levees, floodwalls, and non-structural) were designed to account for the USACE intermediate sea level rise projection through the year 2073 using the joint probability method to account for a range of streamflows, and are expected to provide robust flood risk reduction over the project design life. Based on the findings of this analysis, it is recommended to communicate the potential risks of climate change in the region to the local sponsor for consideration in future city planning recognizing the current design accounts for future changes in sea level rise but may be further affected by future changes in hydrology.

5.0 HYPOTHETICAL RAINFALL

A 48-hour duration hypothetical storm was modeled so that the Rahway River basinwide HEC-HMS model developed for this study would be accurate for times of concentration as large as 24 to 48 hours.

Specific frequency point precipitation estimates in inches were obtained for the Rahway River basin from "Precipitation-Frequency Atlas of the United States" NOAA Atlas 14, volume 2. The data was determined at Cranford, NJ (40.65N, 74.30W) as a representative basin location.

Point rainfall depths were part of the HEC-HMS model input and were converted to finite area rainfall depths with transposition storm areas and procedures contained in HEC-HMS. A time step of 5 minutes was used for the HEC-HMS models because of the sizes and times of concentration of the HEC-HMS model subbasins. The time series data of the hypothetical storms modeled is therefore given in 5-minute increments. The hypothetical point rainfall data for this watershed is given in Table 1. A storm area of 83.13 square miles was used to reduce point rainfall values to finite drainage area values, because it is the drainage area of the Rahway River at its mouth.

Table 1: Rahway River Basin Point Rainfall Depths in Inches for Hypothetical Storms according to NOAA Atlas 14

	1-yr	2-yr	5-yr	10-yr	25-yr	50-yr	100-yr	200-yr	500-yr
5-min	0.34	0.40	0.47	0.52	0.59	0.63	0.68	0.72	0.77
15-min	0.67	0.80	0.96	1.06	1.19	1.28	1.36	1.44	1.53
60-min	1.14	1.39	1.74	2.00	2.35	2.61	2.87	3.14	3.49
2-hr	1.40	1.70	2.16	2.51	3.00	3.41	3.82	4.26	4.87
3-hr	1.56	1.90	2.41	2.81	3.36	3.81	4.28	4.76	5.44
6-hr	2.00	2.44	3.08	3.61	4.36	5.00	5.67	6.39	7.41
12-hr	2.48	3.02	3.84	4.54	5.56	6.43	7.39	8.44	9.96
24-hr	2.81	3.40	4.37	5.19	6.44	7.52	8.72	10.07	12.07
2-day	3.31	4.01	5.12	6.06	7.43	8.60	9.88	11.28	13.32

6.0 STREAMFLOW

6.1 Peak Discharge Records

There are, at present, three active continuous record USGS stream gages in the Rahway River basin.

1. USGS 01394500 Rahway River at Springfield: The gage is located on the left bank of the Rahway River, 50 feet downstream from the bridge on eastbound U.S. Highway 22, 100 feet downstream from Pope Brook and 1.50 miles south of Springfield. The drainage area at the gage is 25.50 square miles and the period of record is from July 1938 to the current year.

- Partially captures Hurricane Irene but the peak flow is estimated.
- Captures Tropical Storm Ida.

2. USGS 01395000 Rahway River at Rahway: The gage is located on the left bank of the Rahway River, 100 feet upstream from the bridge on St. Georges Avenue in Rahway, 0.90 miles upstream from the confluence with Robinsons Branch, and 1.70 miles southwest of Linden. The drainage area at the gage is 40.90 square miles and the continuous period of record is from October 1921 to the current year.

- Partially captures Hurricane Irene, peak is not available.
- Partially captures Tropical Storm Ida, peak and tail are estimated.

3. USGS 01396000 Robinson Branch at Rahway: The gage is located on the right bank of Robinsons Branch, 70 feet upstream of the dam on Milton Lake, 0.40 miles upstream from Maple Avenue at Milton Lake in Rahway, 0.60 miles downstream from Middlesex Reservoir Dam, and 1.60 miles upstream from the mouth. The drainage area at the gage is 21.60 square miles. The gage was a continuous-record gaging station, water years 1937-96. It has been an annual maximum station, water years 1999 to the current year.

- No available data for any of these two storms.

All three gages were used for this watershed. The records of these USGS gaging stations are published in the Water-Data Reports of the U.S. Geological Survey. The locations of these gages and availability of flow data are presented in Figure 3 and Figure 4.

Figure 3. Location and data availability of the USGS stream gages in the Rahway basin
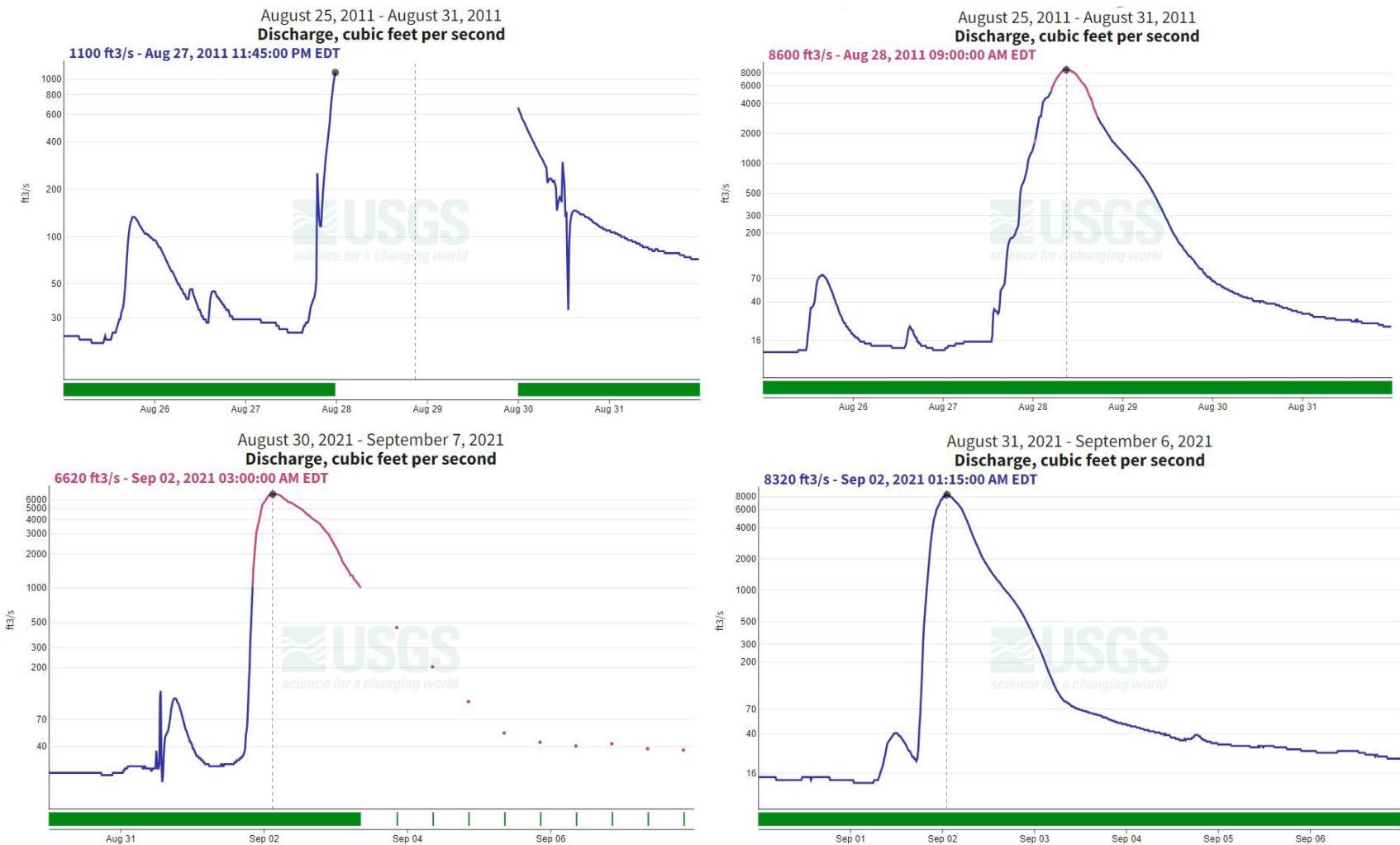
Figure 4. USGS gages flow data for Hurricane Irene (top) and Ida (bottom) at Springfield (right) and Rahway (left)

6.2 Average Discharge

The average annual runoff of the Rahway River basin at the USGS gage near Springfield is 31.40 cfs over the 25.50 square mile drainage area for water years 1939-2009 inclusive or 1.23 cfs per square mile (csm). At the USGS gage at Rahway, the average annual runoff is 50.0 cfs for water years 1922-2009 inclusive over the 40.90 square mile area or 1.23 cfs per square mile (csm). At the USGS gage on Robinsons Branch, the average annual runoff is 22.60 cfs for water years 1939-1980 inclusive over the 21.60 square mile area or 1.05 cfs per square mile (csm). The runoff is equal to an equivalent depth of 16.70 inches per year over the watershed at Springfield and Rahway and 14.20 inches at Robinsons Branch. The average Rahway River basin annual rainfall is 50.94 inches. The runoff at Rahway is equivalent to 32.80 percent of this rainfall.

7.0 HYDROLOGIC MODEL

The Hydrologic Modeling System (HEC-HMS) software (Version 4.12), developed by the Hydrologic Engineering Center, Davis, CA, was used to hydrologically model the Rahway River basin. The HEC-HMS model was converted from a HEC-1 model originally developed by the New York District for previous Rahway River basin studies that focused on Springfield and Robinson's Branch (General Reevaluation Report on the Robinsons' Branch of the Rahway River at Rahway, New Jersey Flood Control Study (July 1985), Volume II – Supporting Documentation: Hydrology). This report provides information on how the watershed physical characteristics were developed and where the HEC-1 model was created. This report uses the original USACE HEC-RAS mode as a base model and updates were done to bring it to present conditions. The updates and modifications are as follows.

7.1 Georeferencing the model

As illustrated in Figure 5 the original basin model was configured with a terrain that did not encompass the subbasins extents. To dissociate the original terrain data from the model, the model was reverted to a previous version of HEC-HMS 4.0, which lacks the capability to utilize terrains. Subsequently, the nodes and reaches were re-imported into HMS 4.11 and georeferenced to the new terrain and shapefiles.

The revised georeferenced model possesses the ability to automatically compute slopes, flow paths, time of concentrations, and sub-basin areas using terrain data.
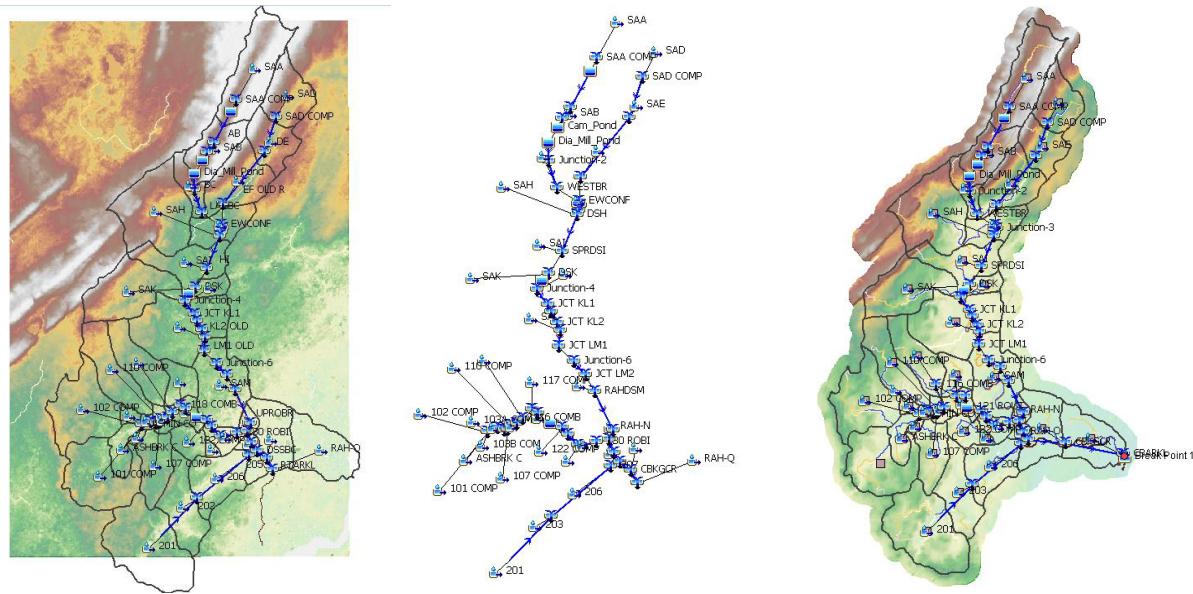
Figure 5. Physical Model in the HEC-HMS Original USACE (left), Disconnected Nodes (middle), AECOM Modified Model (right)

7.2 Meteorological data

The original USACE model utilized data from the three precipitation gauges in the area to derive a weighted average precipitation for each basin. To enhance accuracy, 4km-grid radar data were obtained from the NOAA website and applied to the entire model area.

Precipitation data for Hurricane Irene covers the timeline of 08/27/2011 to 08/31/2011, while data for Tropical Storm Ida spans from 08/31/2021 to 09/05/2021. To compare the impact of the grid precipitation data with the original USACE model, Figure 6 illustrates the overlap comparison in two different sub-basins chosen from the north (SAI) and south (206) of the watershed.
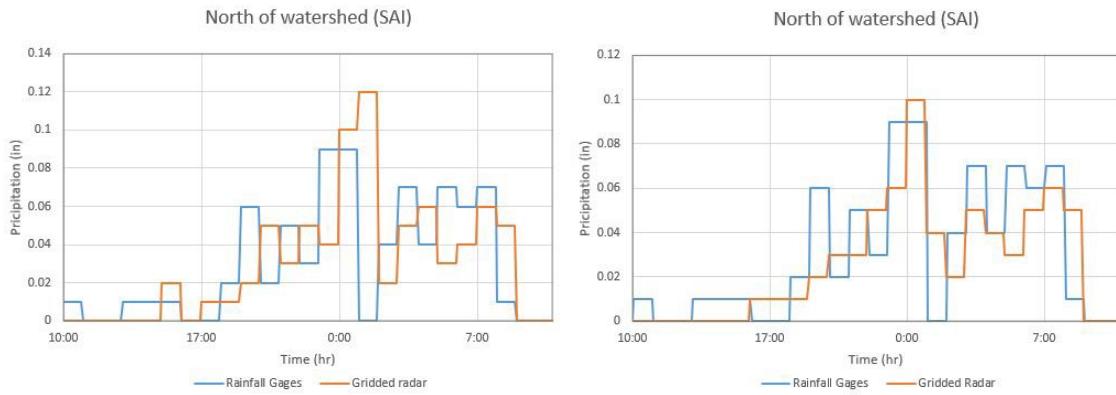
Figure 6. Comparing the precipitation data from the rainfall gages and Gridded radar data

7.3 Dam and spillway structure

The base model employed the Elevation-Storage-Discharge method to simulate the Lenape Park Dam, Orange Reservoir, Campbell Pond, and Diamond Mill Pond. This method uses Elevation-Storage and Storage-Discharge pair graphs to model the dams. For a more detailed and accurate simulation, the simulation approach was changed to the "outflow structure" method and all the physical attributes of the dams, spillways, weir, and culvert applied to the model. On top of providing better results, having the real physical parameters of the structures facilitate easier adjustments for future developments.

7.4 Subbasin data

Figure 7 shows the Rahway Watershed with subbasins, and Figure 8 shows a schematic diagram of the HEC-HMS model. Table 2 gives the name of each element, its description, the drainage area and the type of computation. Subbasin data that includes unit hydrograph parameters and percent impervious/pervious area for the watershed is presented in Table 3. Several methods of channel routing are utilized in the various stream reaches.

Table 4. Existing Conditions Reach Parameters

Reach Node	Lag Time (min)	Muskingum		
		K (hrs)	X	Number of Subreaches
AB		0.6	0.10	1
DE		0.60	0.30	1
104 ROUT		0.50	0.10	1
109 ROUT		0.41	0.10	1
112 ROUT		0.39	0.10	1
202		1.15	0.30	1
205		1.29	0.30	1
LAGAB	15			
LAGBC	15			
LAGCFG	20			

7.5 Reach routing and storage modification

Comparison of the results from the base model with the observed gauge data reveals significant deviations in the calculated dam storage and river routings from the reality of the basin. The base model employed the Elevation-Storage-Discharge method to simulate the Lenape Park Dam, and it does not fully capture its actual effect on the downstream gauge.

To address this discrepancy, modifications were made to the dam's attributes, transitioning from those required for the Elevation-Storage and Storage-Discharge methods to those necessary for the outflow structure method. This entailed adding a culvert outlet and a spillway to accurately represent the dam's configuration. Additionally, the Elevation-Storage function was adjusted to reflect the output results of the HEC-RAS model of the Rahway River. The attributes of the dam, culvert, and spillway are detailed in Figure 9.

Similar modifications were applied to the Orange Reservoir, Campbell Pond, and Diamond Mill Pond. Despite the Elevation-Storage-Discharge parameters of these three dams mimicking the weir structures, the same modifications were implemented to facilitate easier adjustments for future developments. Figure 10 illustrates the characteristics of these three weir structures simulated in the HMS model. Figure 11 depicts the routing relations.

gives values of Muskingum travel time, K and inflow-storage factor X for those reaches that utilize that method as well as values of lag used in the lag routing method encountered in certain other reaches. Modified Puls routing, using storage-outflow data developed from calibrated historic flood event runs with HEC-RAS, was used where possible.
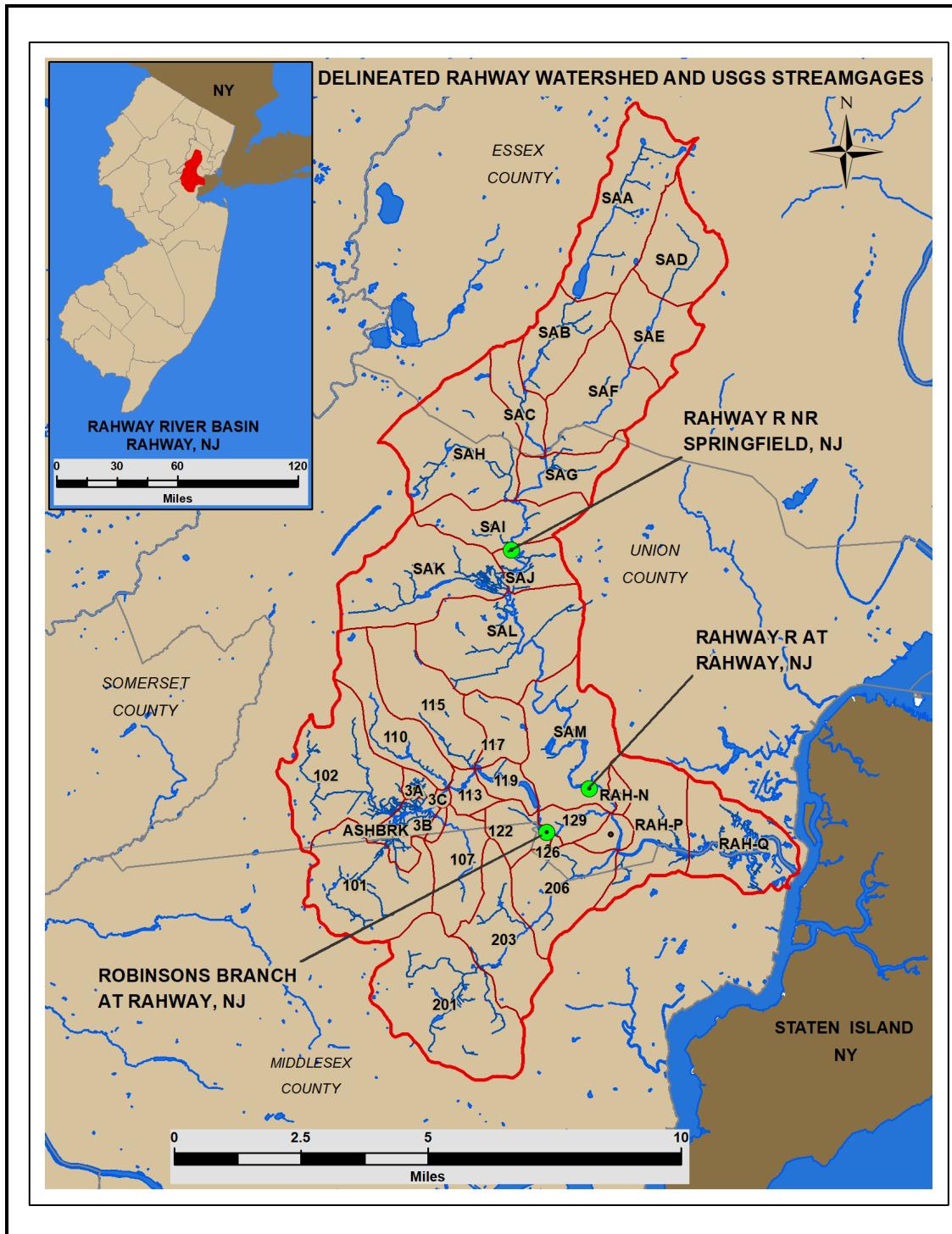
Figure 7. Rahway River Basin with Delineated Subbasins and Stream Gages

Figure 8. Schematic Diagram of HEC-HMS Model
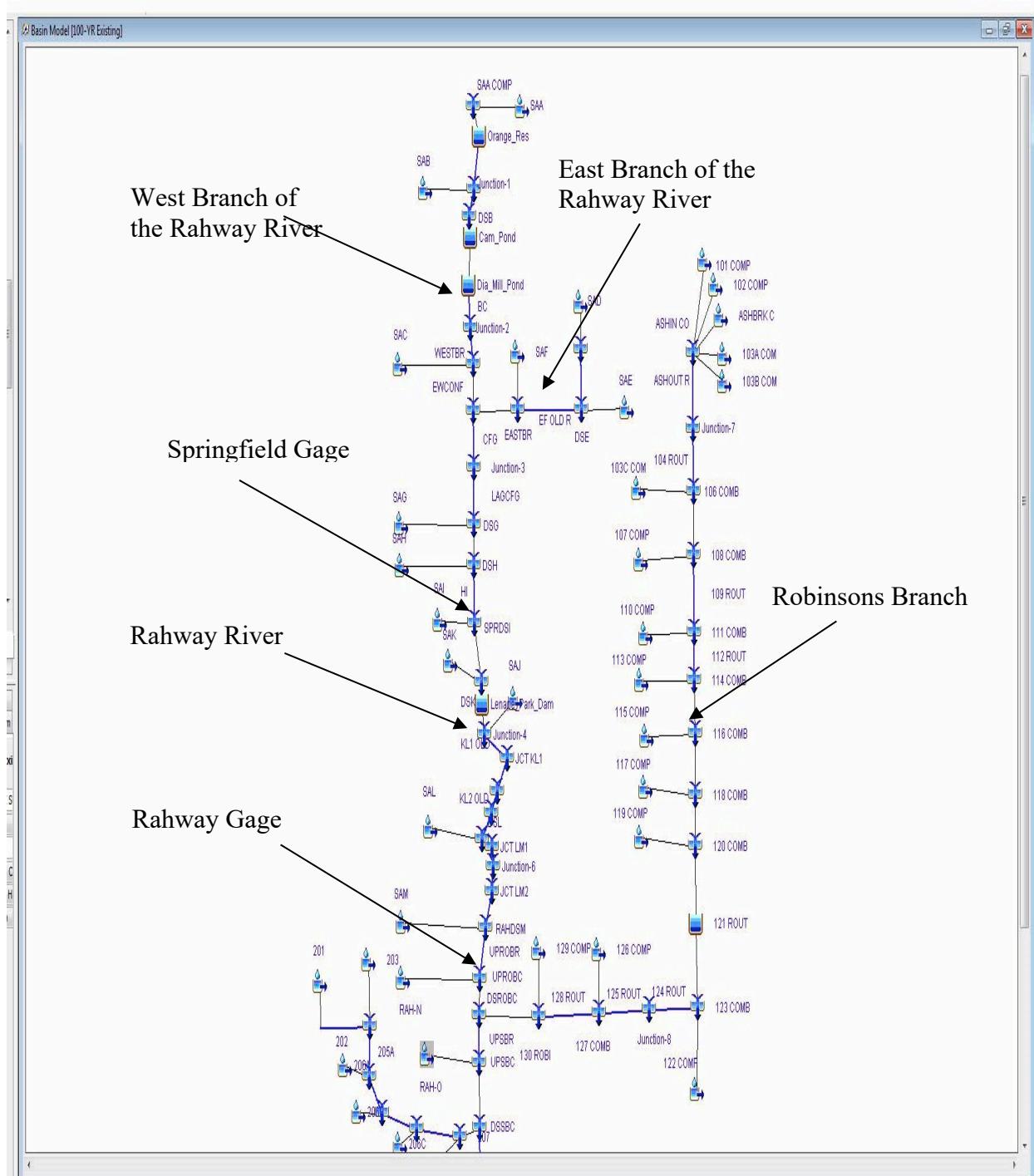
Table 2. HEC-HMS Model Structure, node and basin definitions

Element Name	Element Type	Drainage Area (mi²)	Description
SAA	Subbasin	4.61	Subbasin "A" - W. Branch Rahway Headwaters
SAA COMP	Junction	4.61	Junction "SAA COMP"
Orange_Res	Reservoir	4.61	Orange Reservoir
AB	Reach	4.61	CHANNEL ROUTE THROUGH SOUTH MOUNTAIN RESERVATION
SAB	Subbasin	2.46	Subbasin "B" – South Mountain Reservation
Junction-1	Junction	7.07	W. Branch Rahway Below South Mountain Reservation
LAGAB	Reach	7.07	Lag Routing of Junction-1 Hydrograph
DSB	Junction	7.07	WEST BRANCH RAHWAY AT MILLBURN BELOW DIAMOND MILL POND
Cam_Pond	Reservoir	7.07	Campbell Pond Dam
Dia_Mill_Pond	Reservoir	7.07	Diamond Mill Pond
BC	Reach	7.07	Route thru Millburn
Junction-2	Junction	7.07	Junction-2
LAGBC	Reach	7.07	Lag routing of Junction-2 Hydrograph
SAC	Subbasin	1.12	Subbasin "C" - Millburn
WESTBR	Junction	8.19	W. BRANCH RAHWAY IMMEDIATELY UPSTREAM OF CONFLUENCE
SAD	Subbasin	2.62	Subbasin "D" – East Branch Rahway Headwaters
SAD COMP	Junction	2.62	Junction "SAD COMP"
DE	Reach	2.62	ROUTE THRU SOUTH ORANGE
SAE	Subbasin	2.21	Subbasin "E" - SOUTH ORANGE
DSE	Junction	4.83	EAST BRANCH AT VILLAGE LINE
EF OLD R	Reach	4.83	ROUTE THRU MAPLEWOOD
SAF	Subbasin	3.28	Subbasin "F" - MAPLEWOOD

Element Name	Element Type	Drainage Area (mi²)	Description
EASTBR	Junction	8.11	E. BRANCH RAHWAY IMMEDIATELY UPSTREAM OF CONFLUENCE
EWCONF	Junction	16.30	RAHWAY DOWNSTREAM OF E. AND W. BRANCHES
CFG	Reach	16.30	ROUTE THRU SUBBASIN "G"
Junction-3	Junction	16.30	Junction-3
LAGCFG	Reach	16.30	Lag Routing of Junction-3 Hydrograph
SAG	Subbasin	1.94	Subbasin "G"
DSG	Junction	18.24	RAHWAY AT MILLTOWN
SAH	Subbasin	5.47	Subbasin "H" - VAN WINKLE BROOK AT MOUTH
DSH	Junction	23.71	RAHWAY AT MILLTOWN
HI	Reach	23.71	ROUTE THRU SPRINGFIELD TWP.
SAI	Subbasin	2.84	Subbasin "I"
SPRDSI	Junction	26.55	COMBINED FLOW AT USGS GAGE NEAR SPRINGFIELD
SAK	Subbasin	4.32	Subbasin "K"
DSK	Junction	30.87	COMBINED INFLOW INTO LENAPE PARK
Lenape_Park_Dam	Reservoir	30.87	Lenape Park Levee System with Hydraulic Structure
SAJ	Subbasin	0.75	Subbasin "J"
Junction-4	Junction	31.62	Junction-4
KL1 OLD	Reach	31.62	ROUTE THRU NOMAHEGAN PARK IN CRANFORD
JCT KL1	Junction	31.62	
KL1 1	Reach	31.62	
Junction-5	Junction	31.62	Damage Center in Cranford
KL2 OLD	Reach	31.62	ROUTE THRU CRANFORD TO NJ CENTRAL RAILROAD
JCT KL2	Junction	31.62	
mus_KL2	Reach	31.62	
SAL	Subbasin	5.46	Subbasin "L"

Element Name	Element Type	Drainage Area (mi²)	Description
DSL	Junction	37.08	COMBINED FLOW AT NJ CENTRAL RAILROAD
LM1 OLD	Reach	37.08	ROUTE THRU CLARK TO GARDEN STATE PARKWAY
JCT LM1	Junction	37.08	
mus_LM1	Reach	37.08	
Junction-6	Junction	37.08	Junction-6
LM2 OLD	Reach	37.08	ROUTE THRU CLARK TO USGS GAGE AT RAHWAY
JCT LM2	Junction	37.08	
mus_LM2	Reach	37.08	
SAM	Subbasin	4.11	Subbasin "M"
RAHDSM	Junction	41.19	COMBINED FLOW AT USGS GAGE AT RAHWAY
UPROBR	Reach	41.19	ROUTE HYDROGRAPH AT RAHWAY GAGE TO ROBINSON'S BRANCH CONFLUENCE
RAH-N	Subbasin	0.42	COMPUTE SUBBASIN RAH-N RAHWAY MAINSTREAM RAHWAY GAGE TO ROBINSON'S BRANCH CONFLUENCE
UPROBC	Junction	41.61	COMBINE SUBBASIN RAH-N AND ROUTED HYDROGRAPH OF RAHWAY GAGE AT ROBINSON'S BRANCH CONFLUENCE
102 COMP	Subbasin	4.42	**Robinson's Branch Rahway River subbasin 102**
101 COMP	Subbasin	4.32	Subbasin 101
ASHBRK C	Subbasin	1.11	Ash Brook Swamp subbasin
103A COM	Subbasin	0.31	Subbasin 103 A
103B COM	Subbasin	0.17	Subbasin 103 B
ASHIN CO	Junction	10.33	Robinson's Branch inflow to Ash Brook Swamp
ASHOUT R	Reach	10.33	Robinson's Branch outflow from Ash Brook Swamp
Junction-7	Junction	10.33	Robinson's Branch outflow from Ash Brook Swamp
104 ROUT	Reach	10.33	Route to Pumpkin Patch Brook

Element Name	Element Type	Drainage Area (mi²)	Description
103C COM	Subbasin	0.20	Subbasin 103 C
106 COMB	Junction	10.53	Robinson's Branch upstream of Pumpkin Patch Brook
107 COMP	Subbasin	2.10	Subbasin 107 : Pumpkin Patch Brook
108 COMB	Junction	12.63	Robinson's Branch downstream of Pumpkin Patch Brook
109 ROUT	Reach	12.63	Route to confluence subbasin 110
UPSBC	Junction	64.89	COMBINE UPSTREAM OF SOUTH BRANCH CONFLUENCE
201	Subbasin	6.03	COMPUTE SUBBASIN ONE SOUTH BRANCH BASIN NODE 201
202	Reach	6.03	ROUTE TO NODE 202
203	Subbasin	2.91	COMPUTE SUBBASIN TWO SOUTH BRANCH BASIN NODE 203
204	Junction	8.94	COMBINE NODES 202 AND 203 TO GET NODE 204
205A	Reach	8.94	Route to New Dover Road Bridge
206A	Subbasin	0.35	Increment : to New Dover Road Bridge
Junction-New_Dover_BD	Junction	9.29	
205B	Reach	9.29	Route to upstream end Home Depot culvert
206B	Subbasin	0.69	Increment : New Dover Road Bridge to u/s end Home Depot culvert
Junction-HDCulv_US	Junction	9.98	
205C	Reach	9.98	Lag route through Home Depot culvert
206C	Subbasin	0.02	Increment : Home Depot culvert inflow
Junction-StGeor_BD	Junction	10.00	
205D	Reach	10.00	Route from St. George Avenue Bridge to mouth of South Branch
206D	Subbasin	1.81	Increment : St. George Avenue Bridge to mouth
207	Junction	11.81	COMBINE NODES 205 AND 206 TO GET NODE 207

Element Name	Element Type	Drainage Area (mi²)	Description
DSSBC	Junction	76.70	COMBINE NODE 207 WITH RAHWAY MAINSTREAM
RTKGCR	Reach	76.70	ROUTE TO KINGS CREEK
RAH-P	Subbasin	3.05	COMPUTE SUBBASIN RAH-P RAHWAY MAINSTREAM
CBKGCR	Junction	79.75	COMBINE AT KINGS CREEK
RTARKL	Reach	79.75	ROUTE TO ARTHUR KILL
RAH-Q	Subbasin	3.38	COMPUTE SUBBASIN RAH-Q - RAHWAY MAINSTREAM - KINGS CREEK TO ARTHUR KILL
CBARKL	Junction	83.13	COMBINE AT ARTHUR KILL
110 COMP	Subbasin	2.95	Subbasin 110
111 COMB	Junction	15.58	Robinson's Branch downstream of subbasin 110
112 ROUT	Reach	15.58	Route to confluence subbasin 113
113 COMP	Subbasin	2.63	Subbasin 113
114 COMB	Junction	18.21	Robinson's Branch downstream of subbasin 113
115 COMP	Subbasin	0.52	Subbasin 115
116 COMB	Junction	18.73	Robinson's Branch downstream of subbasin 115
117 COMP	Subbasin	1.23	Subbasin 117
118 COMB	Junction	19.96	Robinson's Branch downstream of subbasin 117
119 COMP	Subbasin	0.87	Subbasin 119
120 COMB	Junction	20.83	Robinson's Branch downstream of subbasin 119
121 ROUT	Reservoir	20.83	Outflow from Middlesex Reservoir
122 COMP	Subbasin	1.04	Subbasin 122
123 COMB	Junction	21.87	USGS gage 01396000 Robinson's Br Rahway River at Rahway : Milton Lake Dam
124 ROUT	Reach	21.87	Route from USGS gage Milton Lake Dam to Maple Avenue
Junction-8	Junction	21.87	

Element Name	Element Type	Drainage Area (mi²)	Description
125 ROUT	Reach	21.87	Route from USGS gage Milton Lake Dam to Maple Avenue
126 COMP	Subbasin	0.20	Subbasin 126 : Milton Lake Dam to Maple Avenue
127 COMB	Junction	22.07	USGS gage 01396000 Robinson's Branch Rahway River at Maple Ave in Rahway NJ
128 ROUT	Reach	22.07	Route to mouth of Robinson's Branch
129 COMP	Subbasin	0.85	Subbasin 129 : Maple Avenue to mouth
130 ROBI	Junction	22.92	Robinson's Branch Rahway River at mouth
DSROBC	Junction	64.53	COMBINE UPPER RAHWAY BASIN AND ROBINSON'S BRANCH BASIN AT CONFLUENCE
UPSBR	Reach	64.53	ROUTE TO SOUTH BRANCH CONFLUENCE
RAH-O	Subbasin	0.36	COMPUTE SUBBASIN RAH-O RAHWAY MAINSTREAM - ROBINSON'S BRANCH CONFLUENCE TO SOUTH BRANCH CONFLUENCE

Table 3. Existing Conditions Input Parameters

Subbasin	Drainage Area (mi²)	Percent Impervious (%)	Clark Unit Hydrograph Parameters	
			Time of Concentration Tc (hr)	Storage Coefficient R (hr)
SAA	4.61	25.40	1.00	1.63
SAB	2.46	5.30	1.12	2.07
SAC	1.12	36.90	1.00	0.94
SAD	2.62	39.80	2.40	4.44
SAE	2.21	37.20	1.94	3.60
SAF	3.28	34.10	2.31	4.29
SAG	1.94	39.60	2.54	4.72
SAH	5.47	32.90	1.72	3.19
SAI	2.84	40.50	2.41	4.48
SAK	4.32	37.40	2.90	5.37
SAJ	0.75	31.30	2.10	3.89
SAL	5.46	21.00	2.88	5.35
SAM	4.11	35.50	3.00	5.57
RAH-N	0.42	37.40	1.24	2.29
102 COMP	4.42	27.90	0.97	5.04
101 COMP	4.32	25.20	1.18	5.76
ASHBRK C	1.11	19.30	0.58	3.29
103A COM	0.31	12.10	0.50	2.89
103B COM	0.17	8.70	0.51	3.47
103C COM	0.20	35.00	0.55	3.63
107 COMP	2.10	34.40	0.74	4.26
110 COMP	2.95	30.00	0.75	4.30
113 COMP	2.63	32.00	0.50	3.20
115 COMP	0.52	38.60	0.66	3.98
117 COMP	1.23	41.20	0.50	3.37
119 COMP	0.87	30.20	0.50	2.84
122 COMP	1.04	28.60	0.50	3.36
126 COMP	0.20	29.60	0.50	2.47
129 COMP	0.85	40.90	0.50	3.09
RAH-O	0.36	52.60	1.40	2.60
201	6.03	37.30	3.07	5.69
203	2.91	34.60	2.95	5.46
206	2.87	35.10	4.04	7.47
RAH-P	3.05	54.40	2.91	5.38
RAH-Q	3.38	38.10	4.24	7.85

Table 4. Existing Conditions Reach Parameters

Reach Node	Lag Time (min)	Muskingum		
		K (hrs)	X	Number of Subreaches
AB		0.6	0.10	1
DE		0.60	0.30	1
104 ROUT		0.50	0.10	1
109 ROUT		0.41	0.10	1
112 ROUT		0.39	0.10	1
202		1.15	0.30	1
205		1.29	0.30	1
LAGAB	15			
LAGBC	15			
LAGCFG	20			

7.6 Reach routing and storage modification

Comparison of the results from the base model with the observed gauge data reveals significant deviations in the calculated dam storage and river routings from the reality of the basin. The base model employed the Elevation-Storage-Discharge method to simulate the Lenape Park Dam, and it does not fully capture its actual effect on the downstream gauge.

To address this discrepancy, modifications were made to the dam's attributes, transitioning from those required for the Elevation-Storage and Storage-Discharge methods to those necessary for the outflow structure method. This entailed adding a culvert outlet and a spillway to accurately represent the dam's configuration. Additionally, the Elevation-Storage function was adjusted to reflect the output results of the HEC-RAS model of the Rahway River. The attributes of the dam, culvert, and spillway are detailed in Figure 9.

Similar modifications were applied to the Orange Reservoir, Campbell Pond, and Diamond Mill Pond. Despite the Elevation-Storage-Discharge parameters of these three dams mimicking the weir structures, the same modifications were implemented to facilitate easier adjustments for future developments. Figure 10 illustrates the characteristics of these three weir structures simulated in the HMS model. Figure 11 depicts the routing relations.

Figure 9. Lenape park dam characteristics. Culvert (left), dam storage (top-right), and spillway (bottom-right)

Figure 10. Weir characteristics applied to the Orange Reservoir (top), Campbell Pond (bottom-left), and Diamond Mill (bottom-right)
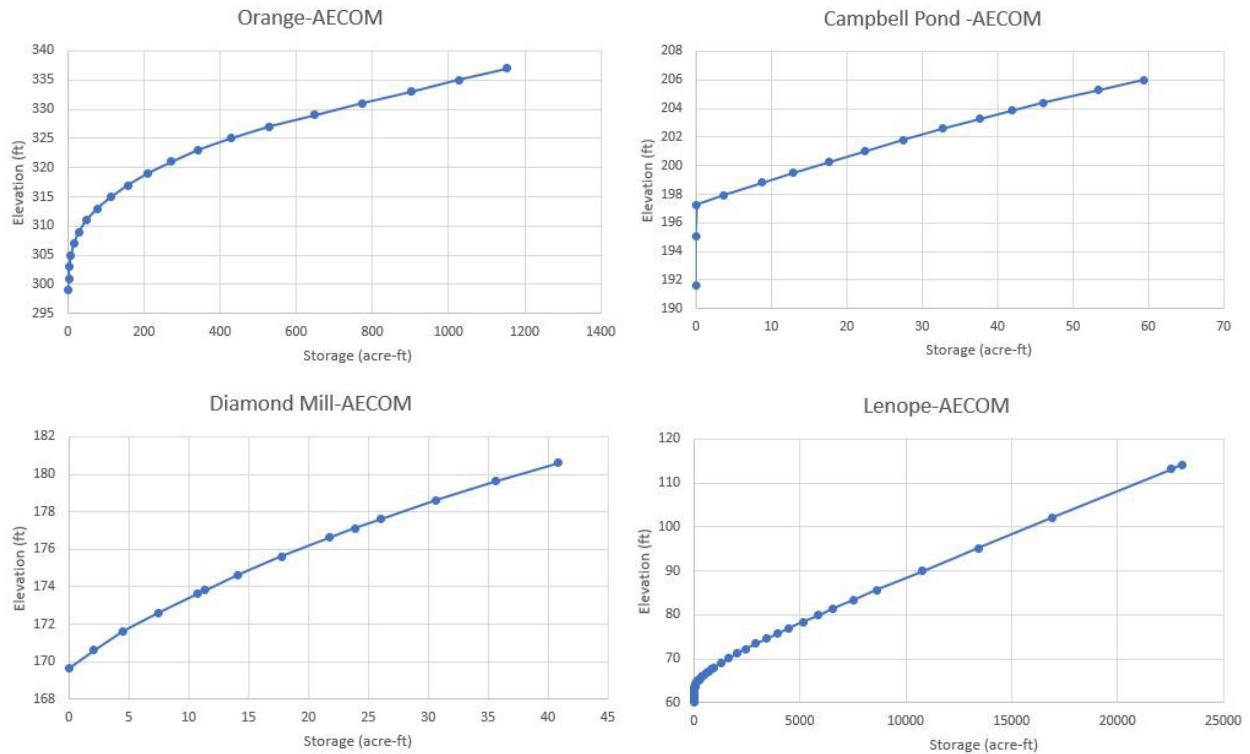
Figure 11. Reservoir routing relations

The results from the base model also indicate a delay in peak flow, occurring hours after the observed peak flow at the gauging stations.

To address this discrepancy, three different methods were employed to calculate the routing for the reaches, namely the Modified Puls, Muskingum, and Lag methods. As a preliminary step, the routing parameters of these methods were adjusted to expedite the routing pace. These modifications yielded significant improvements in the results, bringing the flow hydrographs much closer to the observed data. Subsequently, the exact routing parameters will be extracted from the HEC-RAS model to ensure a more accurate representation of routing in the reaches.

8.0 RECENT LARGE HISTORIC FLOOD CALIBRATION

An HEC-HMS model was used to develop the hydrology of the Rahway River Watershed. The hydrologic analysis for this watershed was completed and was calibrated to the Tropical Cyclone Irene in August 2011 (Section 4.5.3: Tropical Cyclone Irene) and Hurricane Ida in September 2021 (Section 4.5.5: Hurricane Ida). Observed and computed hydrographs, with their associated hyetographs, for the calibration floods at the stream gages are shown in Figure 12 to Figure 15. Also, Table 5 to Table 8 present the numerical comparison between the peak timing, peak flow, and total volume of runoff recorded and computed at each gage.
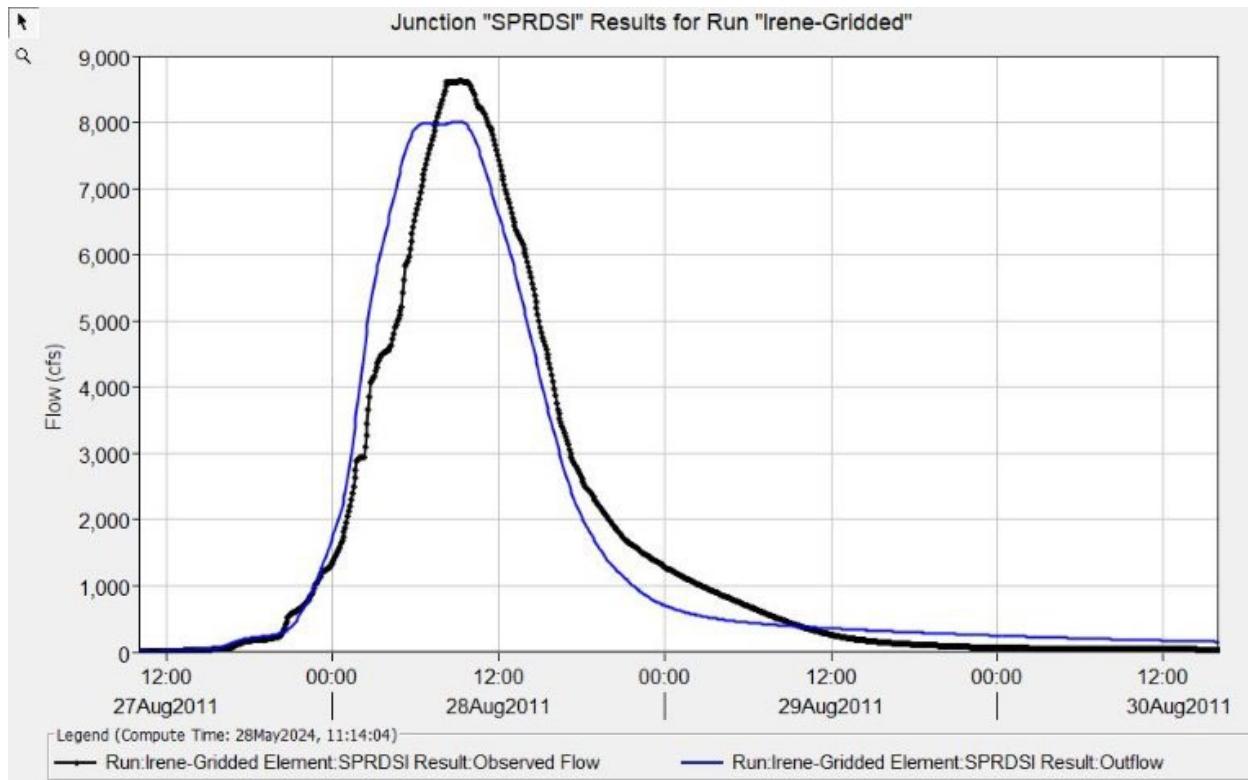
Figure 12. The flow hydrograph at the Springfield gage during Hurricane Irene, comparing the observed and calculated flow

Table 5. Peak flow, peak timing, and total volume during Irene at Springfield gage

Peak Flow	Peak (cfs)	Peak time	Volume (Acre-ft)
Observed	8620	9:15	10448
Calibrated Model	8009 (-7%)	9:05	10434 (-0.2%)
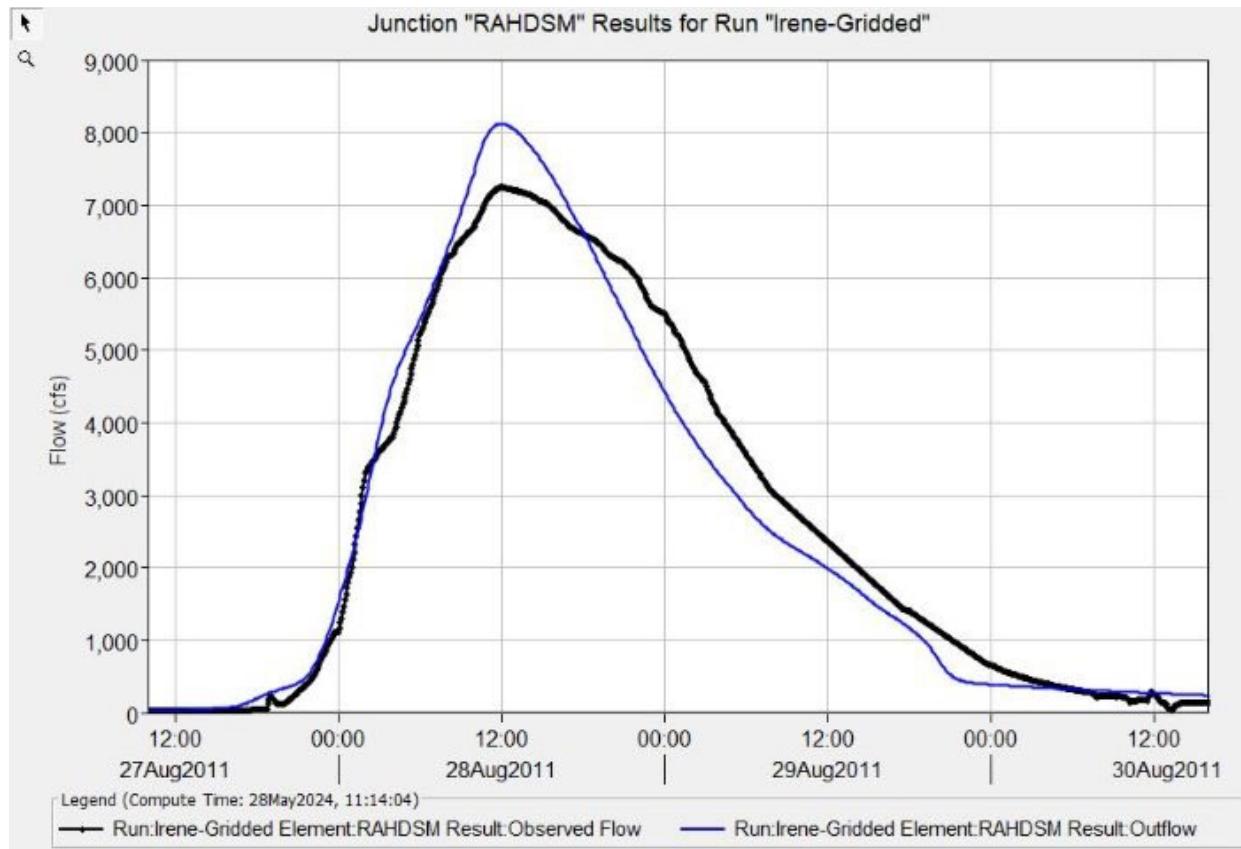
Figure 13. The flow hydrograph at the Rahway gage during Hurricane Irene, comparing the observed and calculated flow

Table 6. Peak flow, peak timing, and total volume during Irene at Rahway gage

Peak Flow	Peak (cfs)	Peak time	Volume (Acre-ft)
Observed	7250	12:00	17040
Calibrated model	8121 (+12%)	12:00	16466 (-3%)
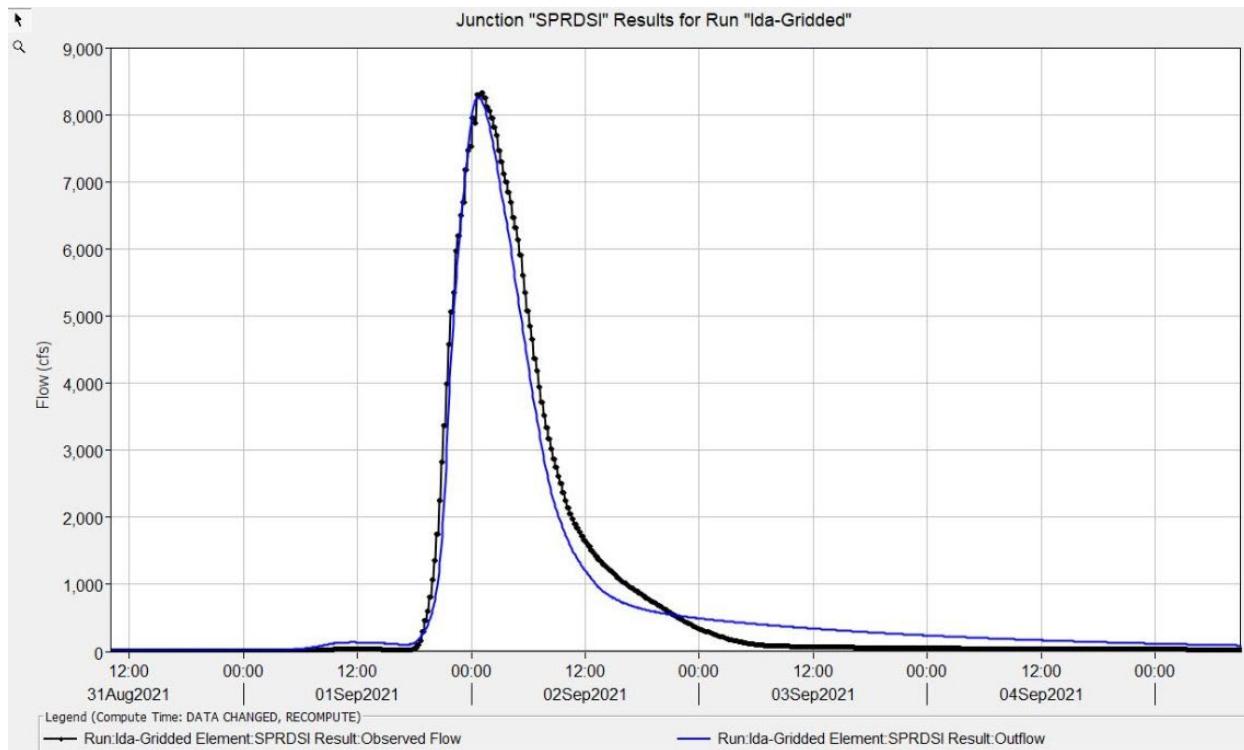
Figure 14. The flow hydrograph at the Springfield gage during Hurricane Ida, comparing the observed and calculated flow

Table 7. Peak flow, peak timing, and total volume during Ida at Springfield gage

| Peak Flow	Peak (cfs)	Peak time	Volume (Acre-ft)
Observed	8320	01:05	7876
Calibrated model	8254 (-1%)	00:45	7922 (+0.5%)
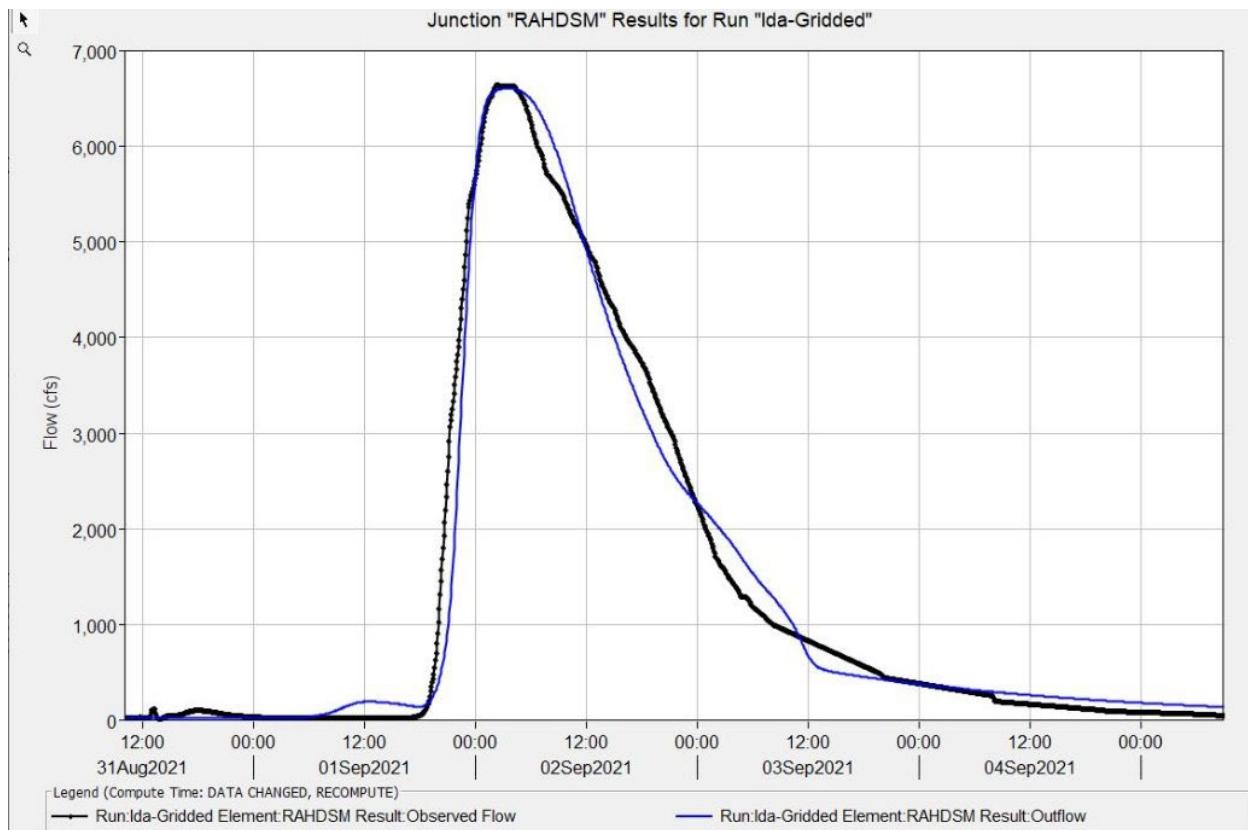
Figure 15. The flow hydrograph at the Rahway gage during Hurricane Irene, comparing the observed and calculated flow

Table 8. Peak flow, peak timing, and total volume during Ida at Rahway gage

Peak Flow	Peak (cfs)	Peak time	Volume (Acre-ft)
Observed	6630	02:15	13283
Calibrated model	6603 (-0.5%)	03:25	13207 (-0.6%)

9.0 CALIBRATION SUMMARY

The calibration process was conducted for two different types of storms, and the parameters used to calibrate the model varied for each of these storms.

Considering the unusual nature of Hurricane Irene, which occurred a few days after another significant rainfall event, it would be conservative to regard the loss parameter used to calibrate the model for Irene as representative of the general condition of the basin.

The parameters utilized to calibrate the model for the dry summer situation of Hurricane Ida are deemed to be a better assumption for the typical conditions of the basin.

Furthermore, the base model significantly overestimated the reach storage capacity, resulting in significant delays in the peak timing of the hydrographs. Consequently, although the base model accurately predicts the peak flow, it is not considered reliable as the prolonged slowing down of the flow in the river does not accurately reflect the nature of the basin. Therefore, adjustments to the base model should be applied to improve its reach routing accuracy.

These routing parameters were adjusted and calibrated using the parametric study to achieve an accurate result in both HMS and RAS models. The volume of water and peak timing were calibrated in the HMS model, while the stage hydrograph calibration was performed in the RAS model.

Some adjustments to the time of concentrations were necessary to the subcatchments in the vicinity of the East Branch. The list of modifications is included in an attachment to this report.

10.0 EXISTING CONDITIONS PEAK DISCHARGE: SPECIFIC-FREQUENCY HYPOTHETICAL FLOODS (CALIBRATION & COMPUTATIONS)

To assess the model's accuracy in predicting peak flow for future hypothetical storms, various frequency rainfall events were incorporated into the model's precipitation storms sections. These events' intensities were sourced from the NOAA Atlas 14 Precipitation Frequency Estimates website in GIS Compatible Format. This data provides the probable rainfall intensity range with 90% confidence for the area of interest and is GIS georeferenced, ensuring each subbasin has a unique dataset. Table 9 outlines the rainfall intensity data for the Rahway basin.

For consistency with the original study and models from the USACE, 48-hour duration hypothetical storms were utilized.

During the calibration of the model for the historical event, it was realized that the loss parameter had to be very different for Irene and Ida. Irene happened a few days after another significant storm which saturated the soil and storages, while Ida happened after a dry season. Considering the nature of the study area, the parameters used to calibrate the model for Ida appear to be more realistic parameters. Therefore, these loss parameters have been used for the hypothetical storm analysis.

The calibrated model was executed for the 99%, 50%, 20%, 10%, 4%, 1%, 0.5%, and 0.2% annual exceedance probability event storms, with the respective peak flows recorded for the Springfield and Rahway gauges.

Additionally, historical peak streamflow data were obtained from the USGS website to analyze the peak flow for the different frequency probability storms. The PeakFQ software from the USGS was utilized for data processing. These historical peak streamflow data are included as three tables in the attachments.

Table 9. NOAA Atlas 14 precipitation frequency estimate

Duration	PDS-based precipitation frequency estimates with 90% confidence intervals (in inches)[1]

	Average recurrence interval (years)
Duration	1	2	5	10	25	50	100	200	500	1000
5-min	0.347 (0.316-0.381)	0.414 (0.377-0.455)	0.492 (0.447-0.540)	0.549 (0.497-0.603)	0.619 (0.558-0.679)	0.671 (0.601-0.737)	0.722 (0.645-0.795)	0.770 (0.683-0.851)	0.831 (0.729-0.924)	0.877 (0.763-0.982)
10-min	0.555 (0.505-0.609)	0.663 (0.604-0.728)	0.788 (0.716-0.865)	0.878 (0.795-0.964)	0.987 (0.890-1.08)	1.07 (0.958-1.17)	1.15 (1.02-1.26)	1.22 (1.08-1.35)	1.31 (1.15-1.46)	1.38 (1.20-1.55)
15-min	0.693 (0.631-0.761)	0.833 (0.759-0.916)	0.997 (0.906-1.10)	1.11 (1.01-1.22)	1.25 (1.13-1.37)	1.35 (1.21-1.49)	1.45 (1.29-1.60)	1.54 (1.37-1.70)	1.65 (1.45-1.84)	1.73 (1.51-1.94)
30-min	0.950 (0.865-1.04)	1.15 (1.05-1.26)	1.42 (1.29-1.56)	1.61 (1.46-1.77)	1.85 (1.67-2.03)	2.04 (1.83-2.24)	2.22 (1.98-2.45)	2.40 (2.13-2.65)	2.63 (2.31-2.93)	2.81 (2.44-3.14)
60-min	1.18 (1.08-1.30)	1.44 (1.32-1.59)	1.82 (1.65-1.99)	2.10 (1.90-2.30)	2.47 (2.22-2.71)	2.76 (2.48-3.03)	3.06 (2.73-3.37)	3.36 (2.98-3.72)	3.78 (3.31-4.20)	4.10 (3.57-4.59)
2-hr	1.44 (1.30-1.58)	1.75 (1.59-1.93)	2.21 (2.01-2.43)	2.57 (2.32-2.82)	3.06 (2.75-3.36)	3.45 (3.09-3.79)	3.86 (3.43-4.25)	4.27 (3.77-4.72)	4.86 (4.23-5.41)	5.32 (4.59-5.96)
3-hr	1.57 (1.42-1.74)	1.92 (1.74-2.12)	2.43 (2.20-2.69)	2.83 (2.55-3.13)	3.39 (3.04-3.74)	3.84 (3.42-4.25)	4.32 (3.81-4.79)	4.82 (4.21-5.35)	5.51 (4.75-6.16)	6.08 (5.17-6.83)
6-hr	1.98 (1.79-2.20)	2.40 (2.17-2.67)	3.03 (2.73-3.36)	3.55 (3.18-3.93)	4.29 (3.82-4.75)	4.91 (4.34-5.44)	5.58 (4.88-6.19)	6.30 (5.45-7.00)	7.34 (6.23-8.21)	8.20 (6.87-9.25)
12-hr	2.39 (2.17-2.68)	2.90 (2.62-3.25)	3.69 (3.32-4.13)	4.36 (3.91-4.87)	5.36 (4.75-5.97)	6.23 (5.48-6.95)	7.18 (6.23-8.01)	8.24 (7.03-9.24)	9.82 (8.21-11.1)	11.2 (9.18-12.7)
24-hr	2.76 (2.54-3.00)	3.33 (3.07-3.64)	4.26 (3.93-4.64)	5.05 (4.64-5.50)	6.24 (5.68-6.76)	7.26 (6.56-7.86)	8.40 (7.51-9.09)	9.66 (8.55-10.5)	11.6 (10.1-12.6)	13.2 (11.3-14.4)
2-day	3.18 (2.92-3.48)	3.85 (3.54-4.22)	4.94 (4.53-5.39)	5.84 (5.34-6.38)	7.18 (6.52-7.81)	8.32 (7.50-9.05)	9.57 (8.56-10.4)	11.0 (9.69-11.9)	13.0 (11.3-14.2)	14.7 (12.7-16.2)
3-day	3.37 (3.12-3.66)	4.08 (3.78-4.44)	5.19 (4.80-5.64)	6.12 (5.64-6.64)	7.48 (6.85-8.10)	8.63 (7.85-9.34)	9.88 (8.92-10.7)	11.2 (10.1-12.2)	13.3 (11.7-14.4)	15.0 (13.1-16.3)
4-day	3.56 (3.31-3.85)	4.30 (4.01-4.65)	5.45 (5.06-5.89)	6.40 (5.93-6.91)	7.78 (7.17-8.38)	8.94 (8.19-9.62)	10.2 (9.28-11.0)	11.5 (10.4-12.4)	13.5 (12.1-14.6)	15.2 (13.5-16.4)
7-day	4.16 (3.88-4.48)	5.00 (4.66-5.39)	6.25 (5.81-6.73)	7.28 (6.75-7.84)	8.78 (8.11-9.44)	10.0 (9.22-10.8)	11.4 (10.4-12.2)	12.9 (11.7-13.8)	15.0 (13.4-16.1)	16.7 (14.9-18.0)
10-day	4.74 (4.44-5.07)	5.67 (5.31-6.07)	6.97 (6.52-7.46)	8.03 (7.50-8.59)	9.54 (8.87-10.2)	10.8 (9.98-11.5)	12.1 (11.1-12.9)	13.4 (12.3-14.4)	15.4 (14.0-16.5)	17.0 (15.3-18.3)
20-day	6.40 (6.05-6.78)	7.60 (7.18-8.05)	9.11 (8.61-9.65)	10.3 (9.74-10.9)	12.0 (11.3-12.7)	13.3 (12.5-14.0)	14.6 (13.7-15.4)	16.0 (14.8-16.9)	17.8 (16.5-18.9)	19.3 (17.7-20.5)
30-day	7.95 (7.55-8.36)	9.38 (8.92-9.87)	11.0 (10.5-11.6)	12.3 (11.7-13.0)	14.1 (13.3-14.8)	15.4 (14.5-16.2)	16.7 (15.7-17.5)	18.0 (16.9-19.0)	19.8 (18.4-20.8)	21.1 (19.6-22.3)
45-day	10.1 (9.67-10.6)	11.9 (11.4-12.5)	13.8 (13.2-14.5)	15.3 (14.5-16.0)	17.1 (16.2-17.9)	18.5 (17.5-19.4)	19.8 (18.7-20.7)	21.1 (19.9-22.1)	22.7 (21.3-23.8)	23.9 (22.4-25.1)
60-day	12.1 (11.6-12.7)	14.3 (13.6-14.9)	16.3 (15.6-17.1)	17.9 (17.1-18.7)	19.9 (19.0-20.8)	21.3 (20.3-22.3)	22.6 (21.5-23.7)	23.9 (22.7-25.1)	25.5 (24.1-26.7)	26.6 (25.1-28.0)

[1] Precipitation frequency (PF) estimates in this table are based on frequency analysis of partial duration series (PDS).

Numbers in parenthesis are PF estimates at lower and upper bounds of the 90% confidence interval. The probability that precipitation frequency estimates (for a given duration and average recurrence interval) will be greater than the upper bound (or less than the lower bound) is 5%. Estimates at upper bounds are not checked against probable maximum precipitation (PMP) estimates and may be higher than currently valid PMP values.

Please refer to NOAA Atlas 14 document for more information.

The analysis was conducted for the Springfield and Rahway gauges. Figure 16 shows the results of the analysis for with 95% confidence to depict the range of the possible peak discharge for the different annual exceedance probability for each of these stations. The EMA global analysis option chosen with the Skew option of "Station". As the result of analysis, the Skew (G) was 1.19 with mean sq error of 0.179.
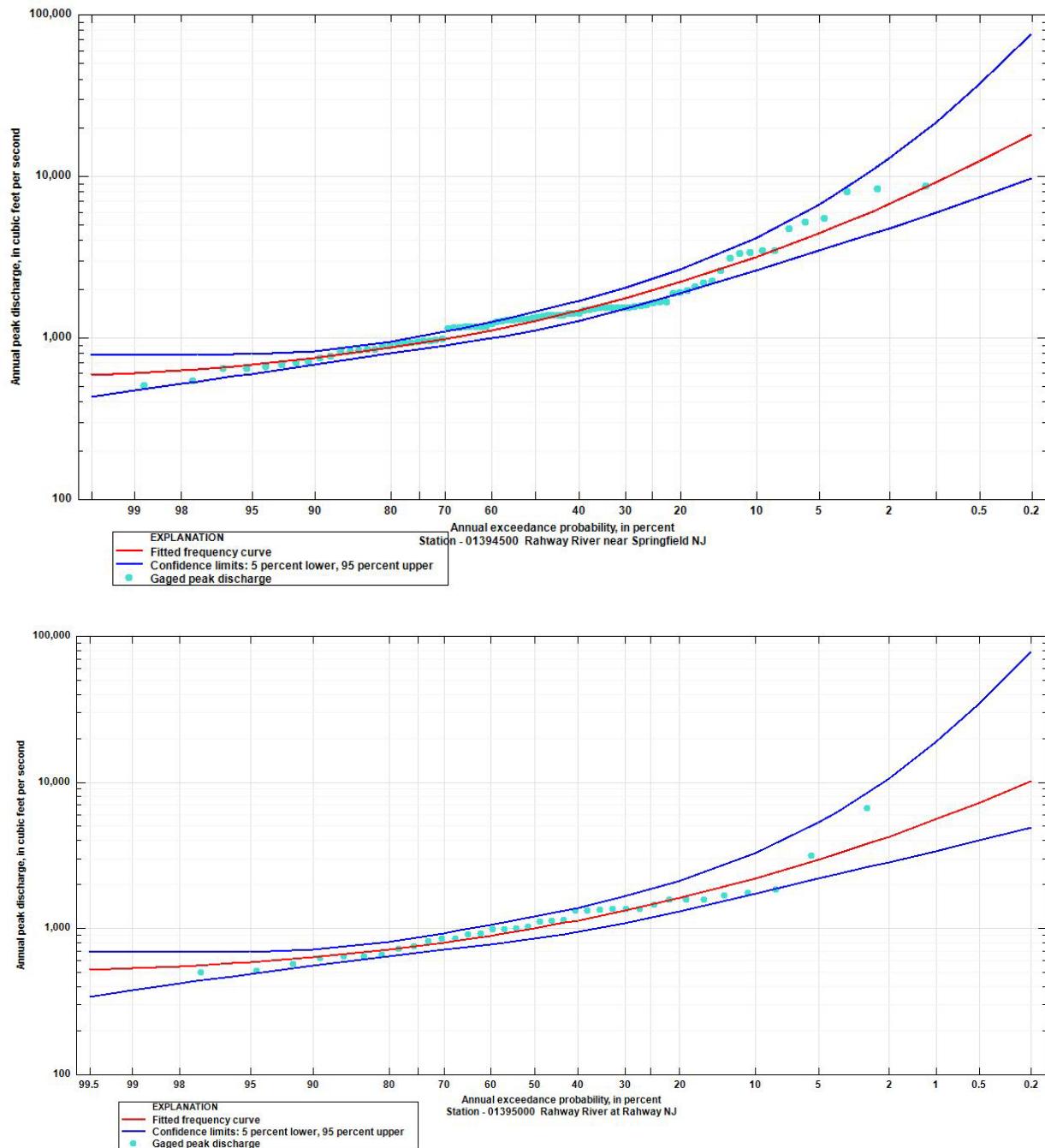
Figure 16. The Peak FQ frequency storm peak analysis for the Springfield gage (top) and Rahway gage (bottom)

For the next step, the hypothetical runs were completed for the different return periods in the HMS model and the results were used to produce similar graphs in the PeakFQ. Figure 17 provides a

comparison between the PeakFQ results and the peak flows of the base model and the calibrated model.
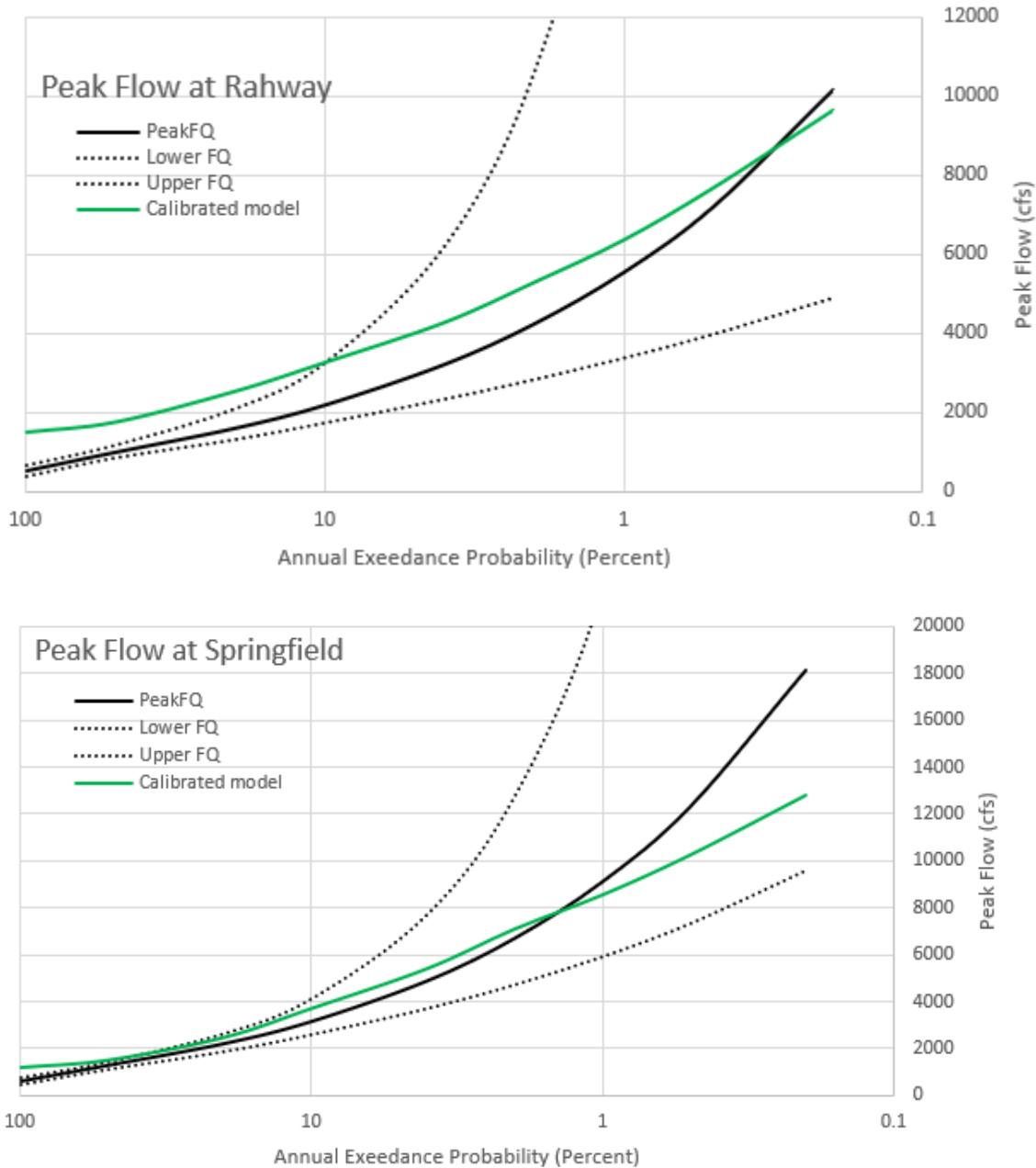
Figure 17. Hypothetical frequency storms result comparison at Rahway (Top) and Springfield (Bottom)

Figure 17 illustrates how the results of the models fit within the PeakFQ range. The findings indicate a close approximation at the Springfield gauge but generally overshoot at the Rahway gauge. Additionally, the model demonstrates a much better response at lower probabilities compared to more frequent ones, which is reasonable given that the model is primarily calibrated for extreme tropical storms and hurricanes.

The PeakFQ analysis for these two gages exploits data acquired from 1930 to 2023. Considering the significant development that took place in this watershed in the past several decades, the data from the earlier part of the 20th century does not accurately represent the current attributes of the watershed. Even though this 100 year of data is a great tool to analyze for the low frequency events, more recent flow data should be used for more accurate calibration of the higher frequency events. Figure 18 shows how the basin development over time resulted in the increase in the mean annual flow and stage in the river.

Table 10 shows a numerical comparison of these data.
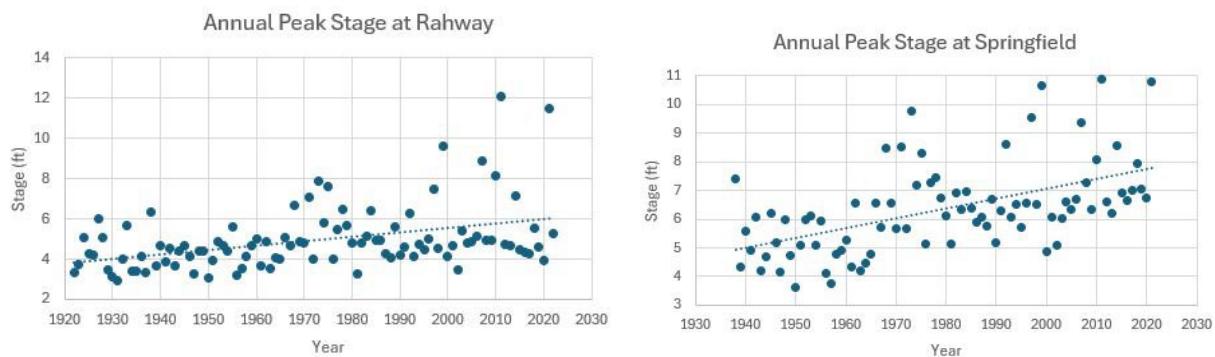
Figure 18. Effect of basin development in the annual flow in the gages

Table 10. Average of flow and stage in the two different scenarios

Gages	Stage Average since 1930	Stage Average since 1984	Flow Average since 1930	Flow Average since 1984
Springfield	6.35	7.04	33.13	38.5
Rahway	4.94	5.57	53.06	62.33

Therefore, another PeakFQ analysis was performed only considering the peak flows from the year 1980 to the present day to achieve a better understanding about the higher frequency results based on the more recent historical data. The result of this analysis is much closer to the results of hypothetical events of the calibrated model.

Table 11 shows the results of the hypothetical storm data from the calibrated model. These results were compared with the results of the PeakFQ analysis for the full duration of the data set and also the analysis for the data after the year 1980.

Even though there are some differences between the result of the hypothetical calibration and PeakFQ analysis, but the numbers are mostly in the confidence band as presented in the Fig. 16 of the report. Considering all the uncertainties in the statistical data, the only noticeable discrepancies is for the high frequency events. Since the PeakFQ analysis performed over the historical data of past 100 years it's logical to expect the development in the watershed and therefore, increase of river's peak flow. It needs to be noted that, the results of the HMS model used as the input of the RAS model. The process of calibrating the model wasn't only focused on the peak flow, but also on the effect of those results on the flood stages in the RAS. A set of optimum parameters needed to be selected to maximize the accuracy in both hydraulic and hydrology models.

Table 11. Hypothetical frequency storms result comparison at Springfield (top) and Rahway (bottom)

Storm Frequency	1-year	2-year	5-year	10-year	25-year	50-year	100-year	200-year	500-year
Peak FQ	598	1270	2190	3130	4870	6680	9090	12280	18110
PeakFQ 1980	817	1480	2582	3802	6211				
Calibrated Model	1197 (+46%)	1505 (+2%)	2470 (-4%)	3709 (-3%)	5415 (+11%)	7109 (+6%)	8566 (-6%)	10269 (-17%)	12829 (-30%)

Storm Frequency	1-year	2-year	5-year	10-year	25-year	50-year	100-year	200-year	500-year
Peak FQ	528	994	1600	2180	3200	4220	5530	7198	10130
PeakFQ 1980	789	1431	2750	4407					
Calibrated Model	1516 (+92%)	1770 (+23%)	2542 (-8%)	3270 (-26%)	4275 (+33%)	5289 (+25%)	6365 (+15%)	7687 (+7%)	9634 (-5%)

11.0 FUTURE UNIMPROVED CONDITIONS HYPOTHETICAL PEAK DISCHARGES

Future conditions hydraulics and hydrology include sea level change, vertical land movement, and urbanization. Figure 19 shows the land use of the Rahway River Watershed in 2020 (present) and 2070 (future) obtained from EPA's Integrated Climate and Land-Use Scenarios (ICLUS) project.

Since the Rahway River basin is so thoroughly developed, the USACE alternate method was adopted to expedite the analysis while producing a reasonable answer. A "worst case scenario" assumption was made that all golf courses and country clubs in the basin would become residentially developed at the same density (average lot size) as adjacent existing residential areas, which were measured using ArcMap. The percent impervious area (RTIMP) of adjacent existing residential areas was determined from their average lot size using a relation in NRCS publication TR-55 (Urban Hydrology for Small Watersheds) as shown in Table 12. Future values of HEC-HMS model subbasin percent impervious area values were then calculated according to this assumption.

HEC-HMS model subbasin Clark unit hydrograph input parameters were predicted to change in response to an increase in their percent impervious area values according to regression equations for time of concentration (T_c) and basin storage coefficient (R) used as a function of subbasin drainage area, slope, and percent impervious area. Subbasin drainage areas and slopes were assumed to remain the same from existing to future conditions.

Table 12 shows the comparison of the impervious area percentage for the current and future conditions.

The models were then run with previously calibrated parameters and only changes in impervious area percentage, T_c, and R. Values of future unimproved conditions peak discharges are shown in Table 13. The result shows the difference between the peak discharges for the existing and future conditions is very similar, especially in the lower frequency events. Based on this finding the decision was to not to move forward with the future analysis of watershed since the difference was negligible.
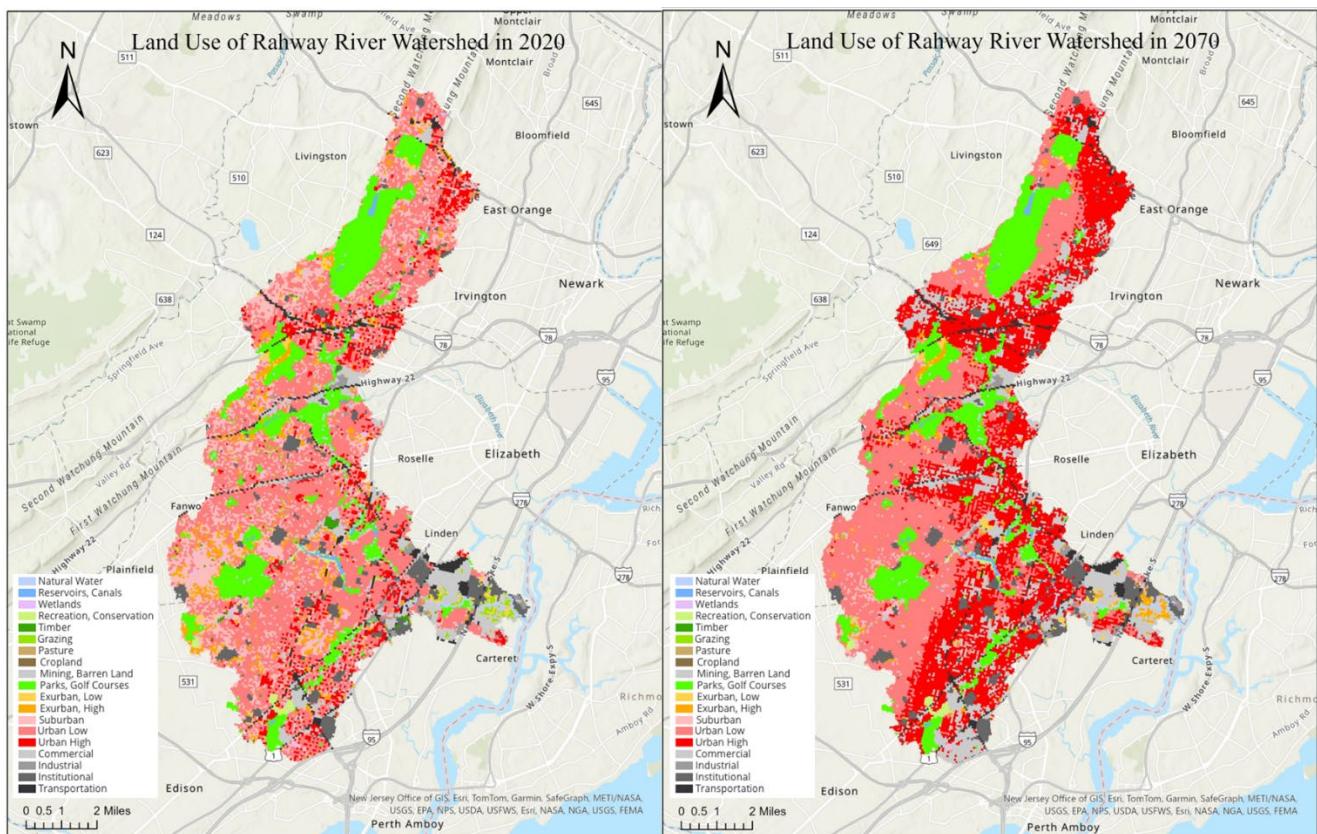
Figure 19. "Without project" present condition inundation map for the 0.1, 0.01, and 0.002 AEP event

Table 12. Impervious area percentage change for the future conditions

Sub	Area (Mi2)	Future Impervious	Current impervious	Percentage change
SAA	4.61	29.9	25.4	4.5
SAB	2.46	5.3	5.3	0
SAC	1.12	36.9	36.9	0
SAD	2.62	40.1	39.8	0.3
SAE	2.21	37.6	37.2	0.4
SAF	3.28	36.7	34.1	2.6
SAG	1.94	39.6	39.6	0
SAH	5.47	34.5	32.9	1.6
SAI	2.84	47.9	40.5	7.4
SAK	4.32	39	37.4	1.6
SAJ	0.75	36.5	31.3	5.2
SAL	5.46	21.1	21	0.1
SAM	4.11	35.6	35.5	0.1
RAH	0.42	37.4	37.4	0
102	4.42	29.34	27.9	1.44
101	4.32	26.14	25.2	0.94
ASH	1.11	19.3	19.3	0
103A	0.31	24.5	12.1	12.4
103B	0.17	27.06	8.7	18.36

103C	0.2	35	35	0
107	2.1	35.89	34.4	1.49
110 COMP	2.95	32.15	30	2.15
113 COMP	2.63	32	32	0
115 COMP	0.52	38.6	38.6	0
117 COMP	1.23	46.16	41.2	4.96
119 COMP	0.87	30.2	30.2	0
122 COMP	1.04	28.6	28.6	0
126 COMP	0.2	29.6	29.6	0
129 COMP	0.85	40.9	40.9	0
RAH-O	0.36	52.6	52.6	0
201 6.03	6.03	38.12	37.3	0.82
203	2.91	34.94	34.6	0.34
206A	0.35	36.5	35.1	1.4
RAH-P	3.05	54.4	54.4	0
RAH-Q	3.38	38.1	38.1	0

Table 13. Peak flow discharges for the Existing and Future undeveloped condition at the Springfield (top) and Rahway (bottom) gages

Storm Frequency	1-year	2-year	5-year	10-year	25-year	50-year	100-year	200-year	500-year
Existing Condition	1185	1492	2436	3634	5345	6991	8401	9988	12341
Future Condition	1278	1609	2599	3800	5596	7251	8672	10340	12829

Storm Frequency	1-year	2-year	5-year	10-year	25-year	50-year	100-year	200-year	500-year
Existing Condition	1501	1759	2512	3201	4254	5280	6350	7610	9529
Future Condition	1573	1838	2595	3294	4361	5400	6486	7789	9747

12.0 PMP ANALYSIS

This section shows the process of applying the HMR52 meteorologic model in HEC-HMS to manually maximize the Probable Maximum Precipitation (PMP) precipitation upstream of Rahway River. The goal is to create a PMF basin model, set up the HMR 52 Storm meteorological model, run a simulation with the PMP event, and then maximize precipitation over a watershed.

The HMR 52 Storm method generates a probable maximum precipitation (PMP) hypothetical storm as detailed in Hydrometeorological Report No. 52. Hydrometeorological Report No. 51 (HMR 51) contains the PMP index maps for the Eastern U.S., and HMR 52 contains information about the application of the PMP depths to a watershed. Figures 18 – 47 in HMR51 contain depth-area-duration (DAD) PMP index values for the area east of the 105th meridian in the United States.

For example, based on Figure 47 of HMR51 (Figure 20), the maximum precipitation for a 72-hr storm in a 20,000 Mi^2 area around central New Jersey is about 14 in.

.
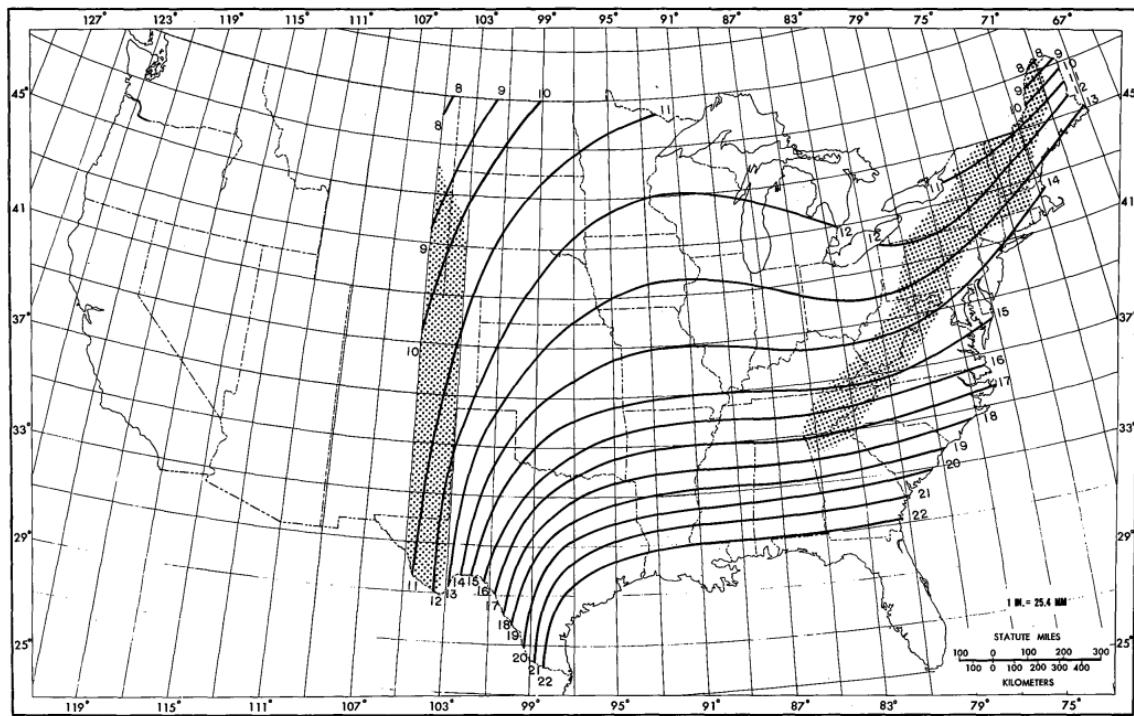
Figure 47.--All-season PMP (in.) for 72 hr 20,000 mi^2 (51,800 km^2).

Figure 20. Example of one of the figures in HMR51

HMR 52 describes a procedure for developing temporal and spatial storm patterns for a 72-hour PMP estimate provided by HMR 51. The HMR 52 method computes a storm area and represents it as elliptical rings of decreasing rainfall intensity. These rings are referenced with a storm center (X and Y coordinates) and basin boundaries. Specifications for the temporal pattern, spatial pattern, storm location, storm area, and storm orientation parameters are applied in accordance with the criteria specified in HMR 52. Initial estimates of each of these parameters are entered by the user. Thereafter, HMS will optimize the parameters to maximize the basin-average precipitation.

Concentric idealized ellipses are used to construct the storm spatial pattern where each ellipse represents an isohyet of precipitation depth. The storm is located over the watershed by specifying the center of the pattern and the angle of the major axis of the ellipses. Total precipitation depth is computed using a specified storm area and area-duration precipitation curves. The total precipitation depth is converted to a temporal pattern based on the selected placement of the peak intensity within the storm duration. The most intense 6-hour period of the storm is constructed using the ratio of precipitation depth between the largest and sixth-largest hours.

The X and Y coordinates specify the location of the storm center and are entered using the same coordinate system as the geometric data for the subbasin polygons. An initial estimate of the West Orange Reservoir provides a good starting point before trying to maximize the PMP by slightly modifying the center coordination. The orientation is measured in degrees increasing clockwise from north (HMR 52 Section 4). The peak intensity parameter specifies the time at which the precipitation intensity will be greatest within the 72-hour storm period (HMR 52 Section 2.3). The depth of rain falling during the period of peak intensity is subdivided into 1-hour increments using the 1 to 6 Ratio parameter (HMR 52 Section 6.5). Finally, the total storm area must be specified. The storm area represents the area of maximum intensity and produces the largest runoff.

By extracting the indexes from the HMR-51 Figures 18 – 47 for the different storm duration and watershed area at the approximate location of Rahway River, Table 14 below was generated.

Table 14. The probable maximum precipitation in (in) for the different watershed area and storm duration for the location of the Rahway basin

		Storm Duration (hr)				
		6	12	24	48	72
Watershed Area (mi2)	10	27	31	34	38	40
	200	18.5	21.5	26	29	30
	1000	13	16.5	21	24	25
	5000	8	11.5	14.5	18	19
	10000	6	9.5	12	15	16.5
	20000	4.5	7.5	10	13	14

To apply these data to the HMS model created for the Rahway project, a PMP meteorological model was created and the HMR52 Storm was chosen as the precipitation calculation method.

Furthermore, the duration-precipitation functions must be added to completely populate the required HMR52 Storm information. These functions are defined as paired data.

Now that the duration-precipitation functions are populated, the HMR52 Storm meteorologic model can be parameterized.

The simulation was completed for the PMP model and by applying parametric study on the center of storm coordination and storm orientation, the precipitation over the watershed maximized. Figure 21 below shows the parameters that lead to the maximum precipitation.

Figure 21. Parameters used to maximize the precipitation over the watershed

After running the model and optimization trial, the maximum PMP at the location of the proposed dams on the West Branch is considered to be 14000 (AC-FT) as shown in Figure 22.
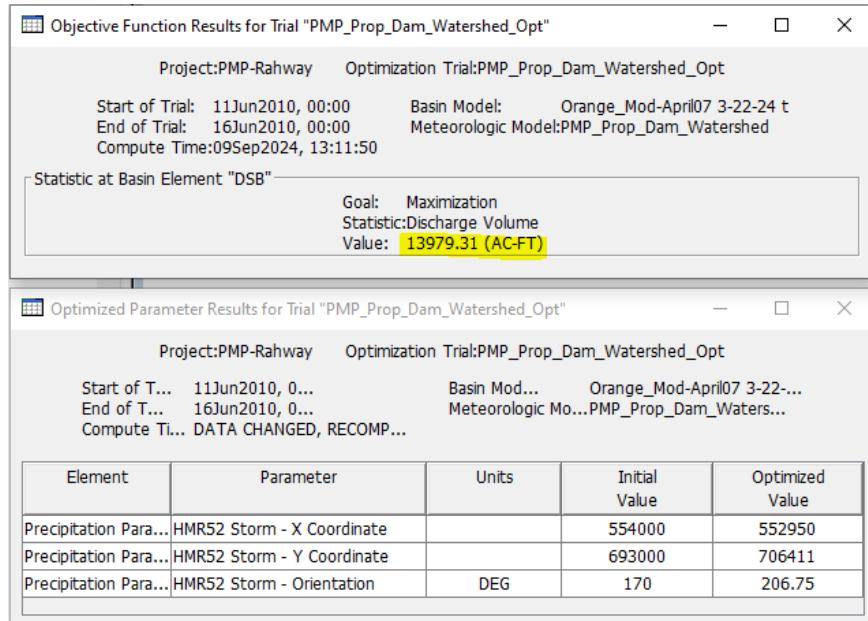
Figure 22. The result of the maximum PMP on the watershed

13.0 ATTACHMENT 1: CLIMATE CHANGE ANALYSIS

Figure 23. 2-digit Water Resources Region Boundaries for the Continental United States, Alaska, Hawaii, and Puerto Rico

	OBSERVED		PROJECTED	
PRIMARY VARIABLE	Trend	Literature Consensus (n)	Trend	Literature Consensus (n)
Temperature	Moderate Increase	Majority report similar trends (8)	Large Increase	Majority report similar trends (10)
Temperature MINIMUMS	Moderate Increase	Low consensus (3)	Moderate Increase	Low consensus (1)
Temperature MAXIMUMS	Moderate Increase	Low consensus (3)	Large Increase	Low consensus (3)
Precipitation	Moderate Increase	Majority report similar trends (12)	Moderate Increase	Low consensus (7)
Precipitation EXTREMES	Moderate Increase	Majority report similar trends (4)	Moderate Increase	Low consensus (3)
Hydrology/Streamflow — Peak Flows			Moderate Increase	Majority report similar trends (8)
Hydrology/Streamflow — Seasonal Shift In Hydrograph	No Change	Majority report similar trends (4)	Moderate Increase	Low consensus (3)
Hydrology/Streamflow — Low Flows			Moderate Increase	Low consensus (2)

TREND SCALE

= Large Increase   = Moderate Increase   = Small Increase   = No Change

= Large Decrease   = Moderate Decrease   = Small Decrease   = No Literature
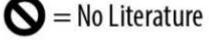
LITERATURE CONSENSUS SCALE

= All literature report similar trend   = Low consensus

= Majority report similar trends   = No peer-reviewed literature available for review

(n) = number of relevant literature studies reviewed

Figure 24. Summary Matrix of Observed and Projected Climate Trends and Literary Consensus

CLIMATE VARIABLE	VULNERABILITY
Increased Ambient Temperatures	Increased ambient air temperatures throughout the century, and over the next century are expected to create the following vulnerabilities on the business lines in the region: • Loss of vegetation from increased periods of drought and reduced streamflows may have impacts on vegetation within the region, which is important for sediment stabilization in the watershed. Loss of non-drought resistant vegetation may result in an increase in sediment loading, potentially causing geomorphic changes in the tributaries to the river system. • Decrease in flows may result from periods of drought and reduced streamflow has implications for maintain water levels in the rivers. **BUSINESS LINES IMPACTED:**
Increased Maximum Temperatures	Air temperatures are expected to increase 2-4°C in the latter half of the 21st century, especially in the summer months. This is expected to create the following vulnerabilities on business lines in the region: • Increased water temperatures leading to water quality concerns, particularly for the dissolved oxygen (DO) levels, growth of nuisance algal blooms and influence wildlife and supporting food supplies. • Increased evapotranspiration. • Human health risk increases from extended heat waves, impacting recreational visitors and increasing the need for emergency management. **BUSINESS LINES IMPACTED:**
Increased Annual Precipitation	By the middle of the century, annual precipitation is expected to increase in the region which are expected to influence the following vulnerabilities on business lines in the region: • Increased flows and runoff, which may carry pollutants to receiving water bodies, decreasing water quality. • Increased erosion with subsequent changes in sediment accumulation rates and creating water quality concerns. • Increased flooding, which may have negative consequences for all infrastructure, habitats, and people in the area. **BUSINESS LINES IMPACTED:**
Increased Storm Intensity and Frequency	Extreme storm events may become more intense and frequent over the coming century which are expected to influence the following vulnerabilities on business lines in the region: • Increased flows and runoff, which may carry pollutants to receiving water bodies, decreasing water quality. • Increased erosion with subsequent changes in sediment accumulation rates and creating water quality concerns. • Change in engineering design standards to accommodate new extreme storms magnitudes. • Increased groundwater recharge rates, as residence times are shortened within areas where evapotranspiration takes place during high intensity events. • Increased flooding, which may have negative consequences for all infrastructure, habitats, and people in the area. **BUSINESS LINES IMPACTED:**
Streamflow Variability	Streamflow will have more extreme variability's by the end of the century. This includes an increase in overall flow, an increase of peak flows, and an increase in low flow levels, which may result in: • Increased flows and runoff, which may carry pollutants to receiving water bodies, decreasing water quality. • Increased erosion with subsequent changes in sediment accumulation rates and creating water quality concerns. • Increased flooding, which may have negative consequences for all infrastructure, habitats, and people in the area. • Loss of vegetation from increased periods of drought and reduced streamflows may have impacts on vegetation within the region, which is important for sediment stabilization in the watershed. Loss of non-drought resistant vegetation may result in an increase in sediment loading, potentially causing geomorphic changes in the tributaries to the river system. • Decrease in flows may result from periods of drought and reduced streamflow has implications for maintain water levels in the rivers. **BUSINESS LINES IMPACTED:**
Sea Level Rise	Sea level rise may exacerbate saltwater intrusion into fresh water supplies. **BUSINESS LINES IMPACTED:**

NOTE: The Regulatory and Military Program business lines may be impacted by all climate variables

= Navigation   = Flood Risk Management   = Ecosystem Restoration   = Hydropower   = Recreation   = Water Supply   = Emergency Management

Figure 25. Summary of Projected Climate Trends and Impacts on USACE Business Lines

Figure 26. Water Resources Region 02-Mid-Atlantic Region Bound

Figure 27. CHAT output using annual instantaneous peak discharge at Rahway River at Rahway, NJ gage; HUC04 Lower Hudson Long Island Basin (0203)

Figure 28. CHAT output using annual instantaneous peak discharge at Rahway River near Springfield, NJ gage; HUC04 Lower Hudson Long Island Basin (0203)
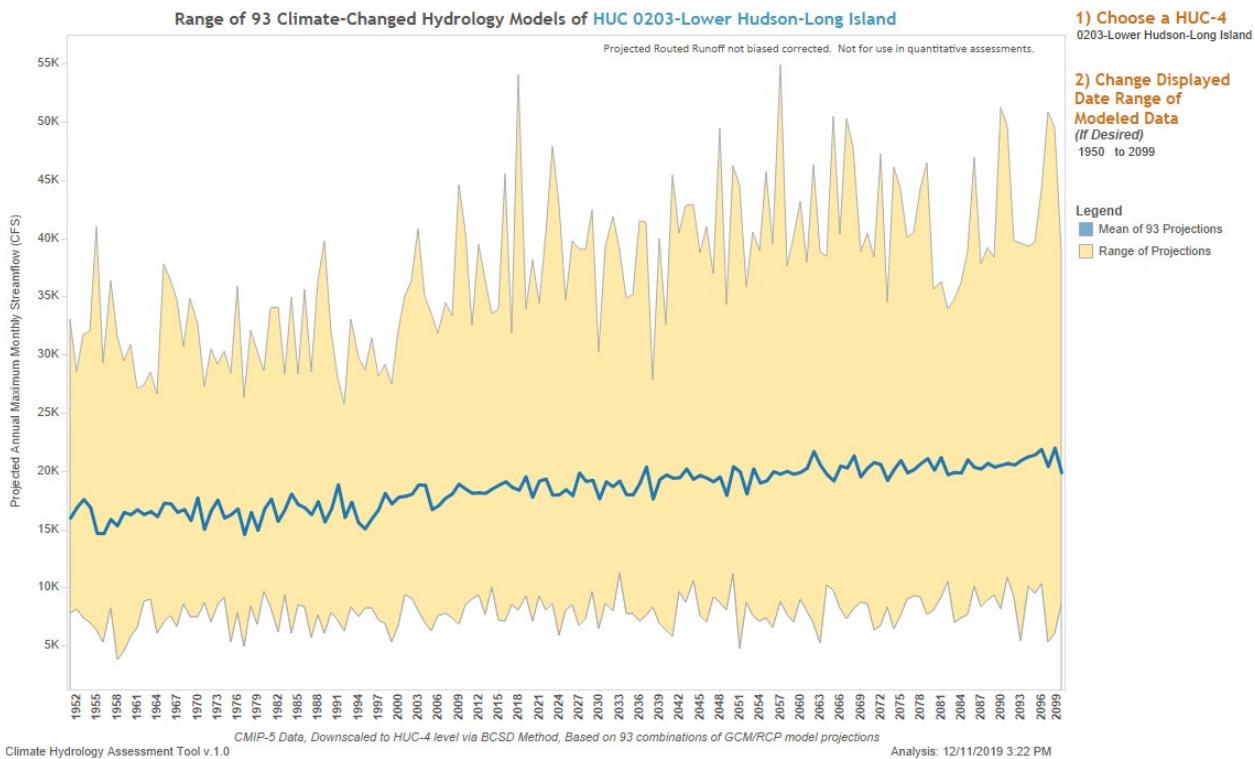
Figure 29. Range of projected annual maximum monthly streamflow in HUC04 Lower Hudson Long Island Basin (0203)
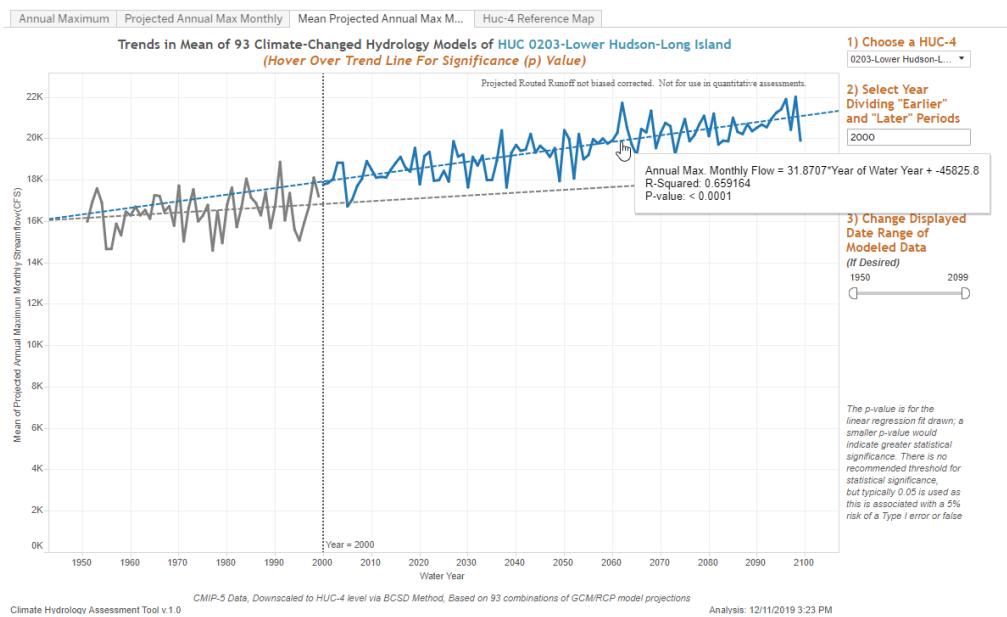
Figure 30. Trends in projected mean annual maximum monthly streamflow; HUC04 Lower Hudson Long Island Basin (0203)
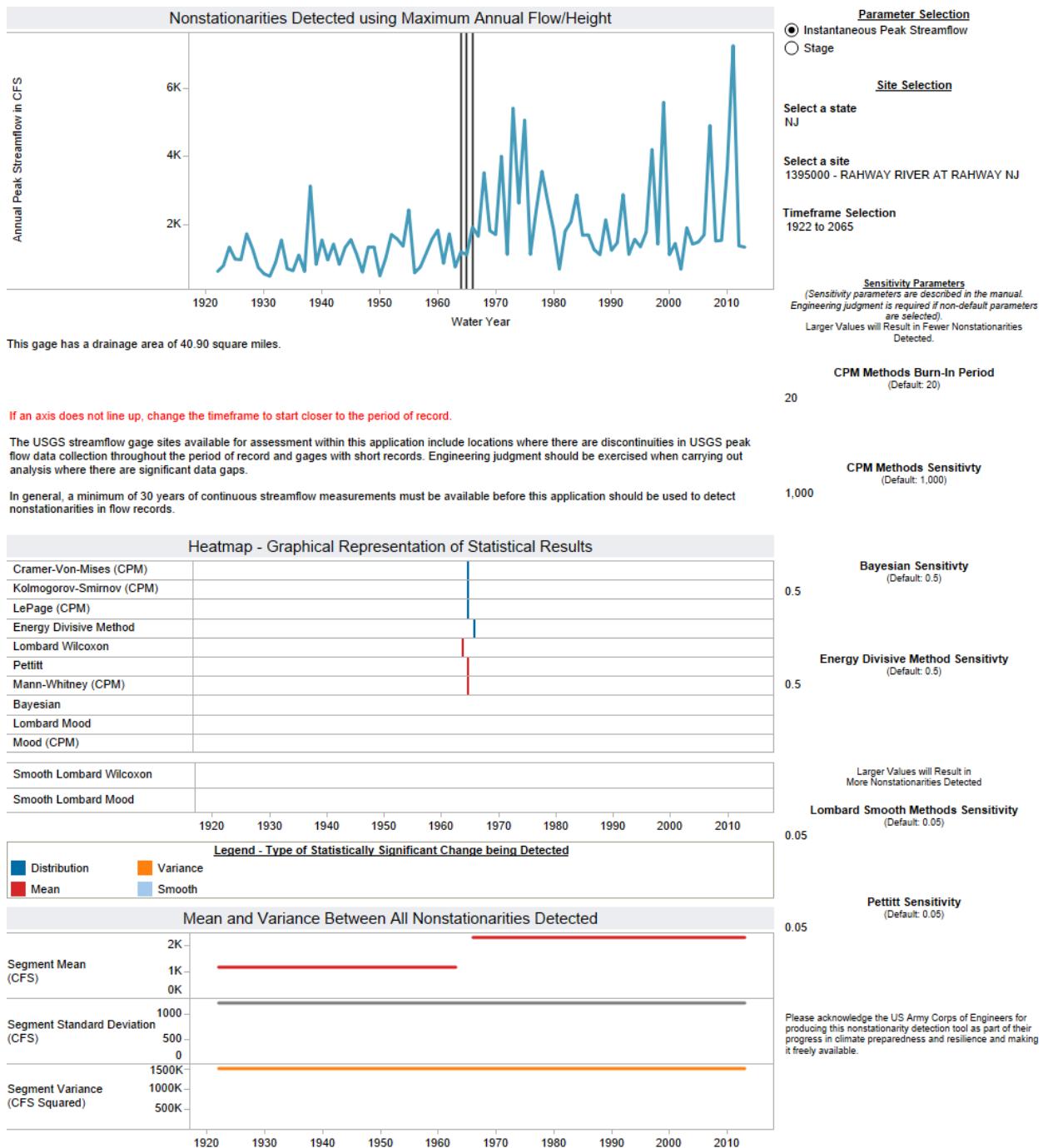
Figure 31. Output from the Nonstationarity Detection Tool – Rahway River at Rahway, NJ
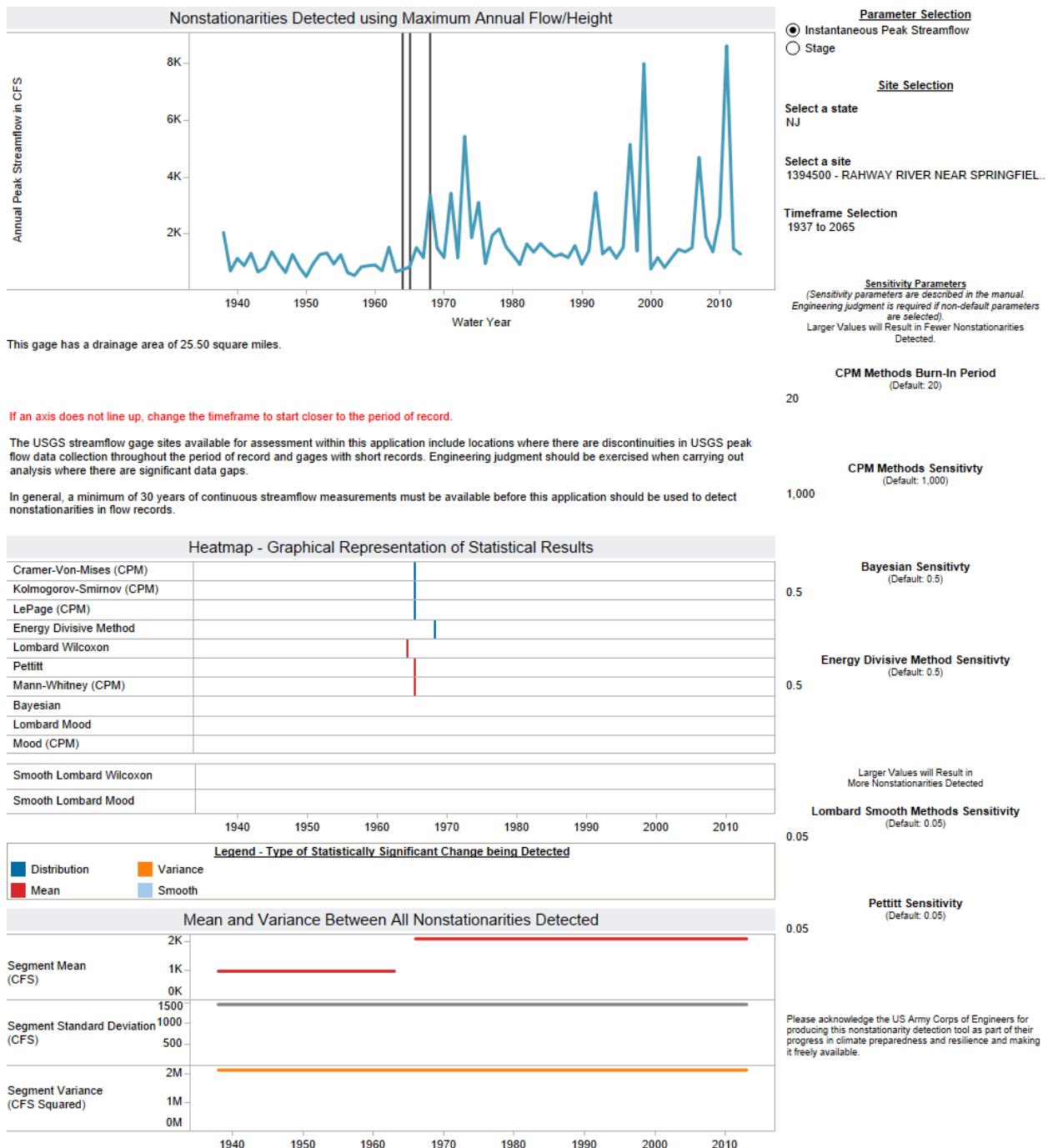
Figure 32. Output from the Nonstationarity Detection Tool – Rahway River near Springfield

Plot of Maximum Annual Flow/Height at
RAHWAY RIVER AT RAHWAY NJ

Timeframe Selection
1965 to 2065
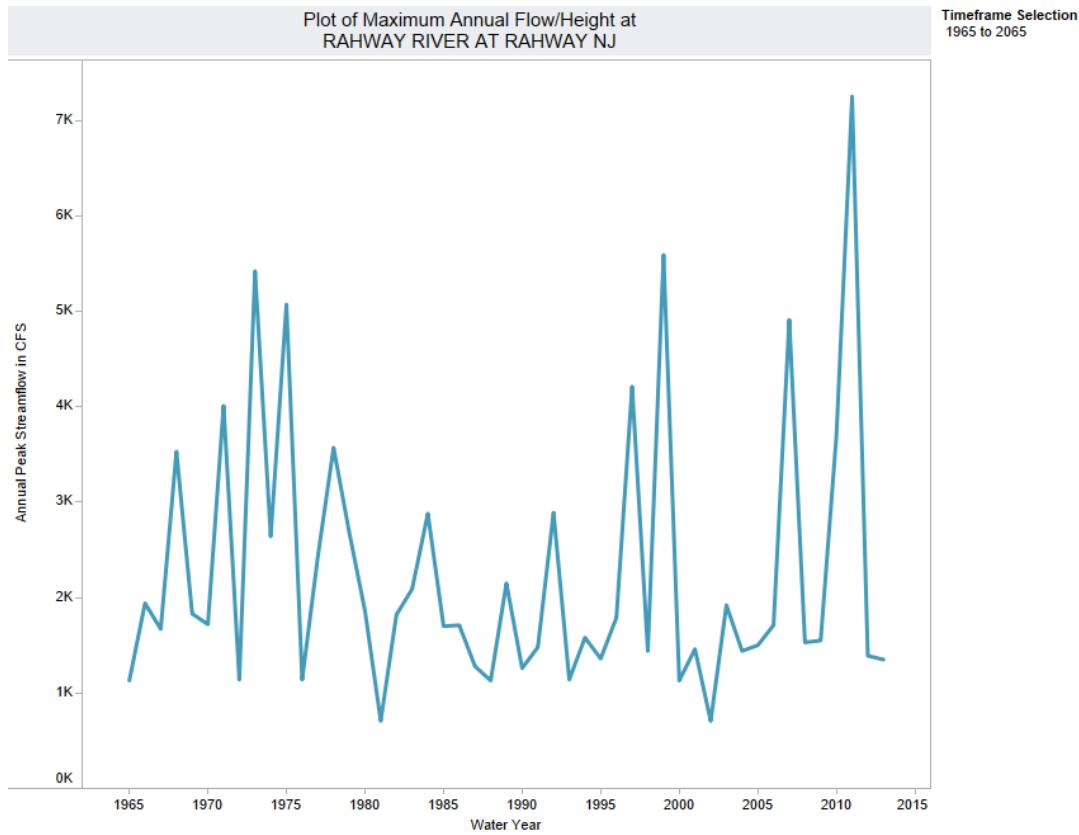
Monotonic Trend Analysis

Is there a statistically significant trend?
No, using the Mann-Kendall Test at the .05 level of significance. The exact p-value for this test was 0.384.
No, using the Spearman Rank Order Test at the .05 level of significance. The exact p-value for this test was 0.388.

What type of trend was detected?
Using parametric statistical methods, **no trend** was detected.
Using robust parametric statistical methods (Sen's Slope), **no trend** was detected.

Please acknowledge the US Army Corps of Engineers for producing this nonstationarity detection tool as part of their progress in climate preparedness and resilience and making it freely available.

Figure 33. Monotonic Trend Analysis – Rahway River at Rahway, NJ

Figure 34. Monotonic Trend Analysis – Rahway River near Springfield, NJ

Table 15. Vulnerability Scores for HUC 0203 for the Flood Risk Reduction Business Line for each scenario-epoch combination nationally, NAD and NAN

Business Line	Scenario-Epoch	WOWA Score	Range Nationally	Range in NAD	Range in NAN
Flood Risk Reduction	Dry – 2050	52.48	35.15-70.08	40.04-52.58	44.36-52.48
	Dry - 2085	53.37	35.15-70.08	40.01-53.37	45.32-53.37
	Wet - 2050	54.42	39.80-92.85	43.13-54.82	48.14-54.42
	Wet - 2085	56.91	39.80-92.85	43.12-56.91	49.69-56.91

Table 16. Values/Percent Contribution to Vulnerability of Each Indicator Associated With the Flood Risk Reduction Business Line for All Scenario-Epoch Combinations along with Percent Changes between Epochs for Each Scenario

Number	Dry-2050	Dry-2085	Percent Change	Wet-2050	Wet-2085	Percent Change
590	25.75/20.95	26.25/20.74	1.95	25.75/19.71	26.25/19.06	1.95
568C	14.046/41.26	14.274/41.61	1.62	15.38/43.06	16.72/43.82	8.69
568L	7.239/18.11	7.340/18.32	2.64	7.952/21.88	8.674/22.29	9.08
277	4.121/16.15	4.165/15.85	1.07	4.098/12.12	3.977/11.64	-2.94
175C	1.326/3.53	1.252/3.47	-5.57	1.240/3.23	1.294/3.20	4.36

14.0 ATTACHMENT 2: SUBBASIN AND REACH PARAMETERS

Subbasin	Initial Loss (IN)	Constant Rate (IN/HR)	Impervious (%)
SAA	3	0.5	25.4
SAB	3	0.5	5.3
SAC	3	0.5	36.9
SAD	3	0.5	39.8
SAE	3	0.5	37.2
SAF	3	0.5	34.1
SAG	3	0.5	39.6
SAH	2.7	0.2	32.9
SAI	2.7	0.2	40.5
SAK	2.7	0.2	37.4
SAJ	2.7	0.2	31.3
SAL	3	0.2	21
SAM	3	0.2	35.5
RAH-N	3	0.017	37.4
102 COMP	3	0.017	27.9
101 COMP	3	0.017	25.2
ASHBRK C	3	0.017	19.3
103A COM	3	0.017	12.1
103B COM	3	0.017	8.7
103C COM	3	0.017	35
107 COMP	3	0.017	34.4
110 COMP	3	0.017	30
113 COMP	3	0.017	32
115 COMP	3	0.017	38.6
117 COMP	3	0.017	41.2
119 COMP	3	0.017	30.2
122 COMP	3	0.017	28.6
126 COMP	3	0.017	29.6
129 COMP	3	0.017	40.9
RAH-O	3	0.017	52.6
201	3	0.017	37.3
203	3	0.017	34.6
206	3	0.017	35.1
RAH-P	3	0.017	54.4
RAH-Q	3	0.017	38.1

Figure 35. Loss parameters for the subbasins

Subbasin	Time of Concentration (HR)	Storage Coefficient (HR)	Time Area Method	Percentage Curve
SAA	1	1.63	Default	
SAB	1.12	2.07	Default	
SAC	1	0.94	Default	
SAD	1.2	4.44	Default	
SAE	1	3.6	Default	
SAF	1.2	4.29	Default	
SAG	1.2	4.72	Default	
SAH	1	3.19	Default	
SAI	2.41	4.48	Default	
SAK	2.9	5.37	Default	
SAJ	2.1	3.89	Default	
SAL	3	6	Default	
SAM	5	7	Default	
RAH-N	1.24	2.29	Default	
102 COMP	0.97	5.04	Default	
101 COMP	1.18	5.76	Default	
ASHBRK C	0.58	3.29	Default	
103A COM	0.5	2.89	Default	
103B COM	0.51	3.47	Default	
103C COM	0.55	3.63	Default	
107 COMP	0.74	4.26	Default	
110 COMP	0.75	4.3	Default	
113 COMP	0.5	3.2	Default	
115 COMP	0.66	3.98	Default	
117 COMP	0.5	3.37	Default	
119 COMP	0.5	2.84	Default	
122 COMP	0.5	3.36	Default	
126 COMP	0.5	2.47	Default	
129 COMP	0.5	3.09	Default	
RAH-O	1.4	2.6	Default	
201	3.07	5.69	Default	
203	2.95	5.46	Default	
206	4.04	7.47	Default	
RAH-P	2.91	5.38	Default	
RAH-Q	4.24	7.85	Default	

Figure 36. Clark Unit Hydrograph parameters for the transfer in the subbasins

Reach	Initial Type	Initial Discharge (CFS)	Muskingum K (HR)	Muskingum X	Number of Subreaches
AB	Discharge = Inflow		0.6	0.10	1
DE	Discharge = Inflow		0.6	0.3	1
104 ROUT	Discharge = Inflow		0.5	0.10	1
109 ROUT	Discharge = Inflow		0.41	0.10	1
112 ROUT	Discharge = Inflow		0.39	0.10	1
202	Discharge = Inflow		1.15	0.3	1
205	Discharge = Inflow		1.29	0.3	1

Figure 37. Muskingum routing parameters for the reaches

Reach	Initial Type	Initial Discharge (CFS)	Stor-Dis Function	Subreaches	Elev-Dis Function	Invert (FT)
BC	Discharge = Inflow		BC OLD R	1	--None--	
EF OLD R	Discharge = Inflow		EF OLD R	1	--None--	
CFG	Discharge = Inflow		CFG	1	--None--	
HI	Discharge = Inflow		HI	1	--None--	
KL1 OLD	Discharge = Inflow		KL1- Aecom	1	--None--	
KL2 OLD	Discharge = Inflow		KL2-AECOM	1	--None--	
LM1 OLD	Discharge = Inflow		LM1-11-14-11	1	--None--	
LM2 OLD	Discharge = Inflow		LM2-AECOM	1	--None--	
UPROBR	Discharge = Inflow		UPROBR	1	--None--	
ASHOUT R	Discharge = Inflow		ASHOUT R	1	--None--	
124 ROUT	Discharge = Inflow		124 ROUT	1	--None--	
125 ROUT	Discharge = Inflow		125 ROUT	1	--None--	
128 ROUT	Discharge = Inflow		128 ROUT	1	--None--	
UPSBR	Discharge = Inflow		UPSBR	1	--None--	
RTKGCR	Discharge = Inflow		RTKGCR	1	--None--	
RTARKL	Discharge = Inflow		RTARKL	1	--None--	

Figure 38. Modified Plus routing parameters for the routing in the reaches

Reach	Initial Type	Initial Discharge (CFS)	Lag Time (MIN)
LAGAB	Discharge = Inflow		15
LAGBC	Discharge = Inflow		15
LAGCFG	Discharge = Inflow		20

Figure 39. Lag parameters for the routing in the reaches

**Table 17. Annual Peak Flows – USGS Gage #1394500 Rahway River near Springfield, NJ
(Based upon COE rating from 1984 Springfield, NJ Hydrology Appendix)**

Water Year	Annual Peak Flow Date	Annual Peak Flows (cfs)	
		Recorded	Adjusted
1938	23 Jul 1938	2050	2825
1939	03 Feb 1939	699	699
1940	31 May 1940	1140	1290
1941	07 Feb 1941	885	930
1942	09 Aug 1942	1320	1600
1943	30 Dec 1942	663	663
1944	13 Mar 1944	815	850
1945	19 Sep 1945	1370	1690
1946	02 Jun 1946	975	1045
1947	05 Apr 1947	646	646
1948	08 Nov 1947	1280	1510
1949	06 Jan 1949	834	865
1950	23 Mar 1950	501	501
1951	30 Mar 1951	954	1020
1952	01 Jun 1952	1280	1510
1953	13 Mar 1953	1330	1635
1954	11 Sep 1954	947	1000
1955	13 Aug 1955	1270	1500
1956	14 Oct 1955	643	643
1957	05 Apr 1957	538	538
1958	28 Feb 1958	844	870
1959	09 Aug 1959	885	930
1960	12 Sep 1960	911	960
1961	16 Apr 1961	708	715
1962	12 Mar 1962	1530	2035
1963	06 Mar 1963	675	680
1964	07 Nov 1963	748	760
1965	08 Feb 1965	838	870
1966	22 Sep 1966	1520	2020
1967	07 Mar 1967	1170	1330
1968	29 May 1968	3370	4330
1969	29 Jul 1969	1510	2000
1970	31 Jul 1970	1170	1330
1971	28 Aug 1971	3430	4390
1972	22 Jun 1972	1160	1390
1973	02 Aug 1973	5430	6130
1974	21 Dec 1973	1870	2590

Water Year	Annual Peak Flow Date	Annual Peak Flows (cfs)	
		Recorded	Adjusted
1975	14 Jul 1975	3110	1400
1976	10 Aug 1976	960	1010
1977	22 Mar 1977	1950	2700
1978	08 Nov 1977	2180	2980
1979	24 Jan 1979	1540	2060
1980	21 Mar 1980	1250	1550
1981	11 May 1981	926	1000
1982	04 Jan 1982	1650	2240
1983	10 Apr 1983	1360	1730
1984	05 Apr 1984	1660	2250
1985	27 Sep 1985	1410	1830
1986	17 Nov 1985	1210	1480
1987	14 Jul 1987	1290	1620
1988	26 Jul 1988	1170	1330
1989	19 Sep 1989	1590	2130
1990	20 Oct 1989	936	1020
1991	04 Mar 1991	1400	1810
1992	05 Jun 1992	3460	4590
1993	01 Apr 1993	1300	1630
1994	28 Jan 1994	1520	2030
1995	18 Jul 1995	1150	1370
1996	19 Jan 1996	1530	2030
1997	25 Jul 1997	5150	5900
1998	02 Apr 1998	1400	1810
1999	16 Sep 1999	7990	7990
2000	18 May 2000	768	768
2001	17 Dec 2000	1170	1330
2002	18 May 2002	824	850
2003	21 Jun 2003	1150	1370
2004	27 Jul 2004	1460	1900
2005	28 Mar 2005	1370	1770
2006	08 Oct 2005	1520	2030
2007	15 Apr 2007	4690	5540
2008	06 Sep 2008	1900	2610
2009	12 Dec 2008	1370	1690
2010	13 Mar 2010	2600	3530
2011	28 Aug 2011	8620	8860
2012	08 Dec 2011	1480	1480
2013	08 Jun 2013	3310	3310

Water Year	Annual Peak Flow Date	Annual Peak Flows (cfs)	
		Recorded	Adjusted
2014	2014-04-30	3,310	3,310
2015	2015-06-15	1,640	1,640
2016	2016-02-25	1,520	1,520
2017	2016-11-29	927	927
2018	2018-04-16	2,220	2,220
2019	2019-07-17	1,560	1,560
2020	2020-07-10	1,370	1,370
2021	2021-09-02	8,320	8,320
2022	2021-10-26	1,580	1,580

Table 18. Annual Peak Flows – USGS Gage #1395000 Rahway River at Rahway, NJ (Based upon pre to post Lenape Park relation from 1984 Springfield, NJ Hydrology Appendix)

Water Year	Annual Peak Flow Date	Annual Peak Flows (cfs)	
		Recorded	Adjusted
1922	19 May 1922	642	540
1923	17 Mar 1923	811	680
1924	07 Apr 1924	1350	1150
1925	12 Feb 1925	1000	830
1926	07 Sep 1926	984	810
1927	02 Aug 1927	1740	1250
1928	06 Jul 1928	1310	1,100
1929	27 Feb 1929	755	630
1930	08 Mar 1930	569	450
1931	29 Mar 1931	500	400
1932	28 Mar 1932	905	750
1933	16 Sep 1933	1560	1300
1934	05 Mar 1934	722	580
1935	06 Oct 1934	660	550
1936	12 Mar 1936	1120	950
1937	20 Dec 1936	640	539
1938	24 Jul 1938	3140	2650
1939	03 Feb 1939	847	700
1940	31 May 1940	1560	1300
1941	07 Feb 1941	976	800
1942	09 Aug 1942	1440	1200
1943	30 Dec 1942	847	700
1944	14 Sep 1944	1340	1120
1945	19 Sep 1945	1570	1310
1946	23 Jul 1946	1140	955
1947	05 Apr 1947	622	520
1948	09 Nov 1947	1350	1150
1949	31 Dec 1948	1350	1150
1950	23 Mar 1950	510	410
1951	31 Mar 1951	1020	840
1952	01 Jun 1952	1720	1430
1953	13 Mar 1953	1590	1350
1954	11 Sep 1954	1380	1160

Water Year	Annual Peak Flow Date	Annual Peak Flows (cfs)	
		Recorded	Adjusted
1955	13 Aug 1955	2440	2030
1956	08 Apr 1956	600	500
1957	06 Apr 1957	770	638
1958	28 Feb 1958	1170	960
1959	09 Aug 1959	1580	1330
1960	12 Sep 1960	1850	1550
1961	23 Mar 1961	878	730
1962	13 Mar 1962	1740	1250
1963	06 Mar 1963	770	638
1964	07 Nov 1963	1210	1000
1965	08 Feb 1965	1130	930
1966	21 Sep 1966	1940	1600
1967	07 Mar 1967	1670	1400
1968	29 May 1968	3530	3030
1969	04 Sep 1969	1830	1540
1970	31 Jul 1970	1720	1430
1971	28 Aug 1971	4010	3540
1972	13 Jul 1972	1140	955
1973	02 Aug 1973	5420	5030
1974	21 Dec 1973	2640	2250
1975	15 Jul 1975	5070	4670
1976	28 Jan 1976	1140	955
1977	23 Mar 1977	2430	2040
1978	08 Nov 1977	3570	3100
1979	24 Jan 1979	2680	2250
1980	28 Apr 1980	1860	1860
1981	12 May 1981	708	708
1982	04 Jan 1982	1820	1820
1983	10 Apr 1983	2090	2090
1984	14 Dec 1983	2880	2880
1985	27 Sep 1985	1700	1700
1986	17 Apr 1986	1710	1710
1987	04 Apr 1987	1280	1280

Water Year	Annual Peak Flow Date	Annual Peak Flows (cfs)	
		Recorded	Adjusted
1988	22 Jul 1988	1130	1130
1989	20 Sep 1989	2150	2150
1990	20 Oct 1989	1260	1260
1991	04 Mar 1991	1480	1480
1992	05 Jun 1992	2890	2890
1993	01 Apr 1993	1140	1140
1994	10 Mar 1994	1580	1580
1995	18 Jul 1995	1360	1360
1996	19 Jan 1996	1790	1790
1997	19 Oct 1996	4210	4210
1998	23 Jan 1998	1440	1440
1999	17 Sep 1999	5590	5590
2000	27 Aug 2000	1130	1130
2001	30 Mar 2001	1460	1460
2002	18 May 2002	706	706
2003	05 Jun 2003	1920	1920
2004	28 Jul 2004	1440	1440
2005	28 Mar 2005	1500	1500
2006	09 Oct 2005	1710	1710
2007	16 Apr 2007	4910	4910
2008	07 Sep 2008	1530	1530
2009	12 Dec 2008	1550	1550
2010	14 Mar 2010	3690	3690
2011	28 Aug 2011	7250	7250
2012	08 Dec 2011	1390	1390
2013	08 Jun 2013	1350	1350
2014	2014-04-30	2,960	2,960
2015	2015-01-18	1,210	1,210
2016	2016-02-25	1,130	1,130
2017	2017-03-31	1,110	1,110
2018	2018-04-16	1,840	1,840
2019	2019-07-23	1,310	1,310
2020	2020-07-11	917	917
2021	2021-09-02	6,630	6,630
2022	2021-10-26	1,680	1,680

Table 19. Annual Peak Flows – USGS Gage #1396000 Robinsons Branch at Rahway, NJ

Water Year	Annual Peak Flow Date	Annual Peak Flows (cfs)
1940	31 May 1940	2856
1941	7 Feb 1941	1669
1942	9 Aug 1942	2394
1943	12 May 1943	1275
1944	6 Jan 1944	1525
1945	19 Sep 1945	1798
1946	2 Jun 1946	1631
1947	5 Apr 1947	916
1948	8 Nov 1947	1806
1949	31 Dec 1948	1472
1950	23 Mar 1950	812
1951	30 Mar 1951	1220
1952	1 Jun 1952	1951
1953	13 Mar 1953	2193
1954	14 Dec 1953	559
1955	13 Aug 1955	1384
1956	8 Apr 1956	701
1957	5 Apr 1957	739
1958	28 Feb 1958	1438
1959	9 Aug1959	1349
1960	12 Sep 1960	1446
1961	23 Mar 1961	1039
1962	12 Mar 1962	1309
1963	6 Mar 1963	720
1964	7 Nov 1963	747
1965	8 Feb 1965	657
1966	21 Sep 1966	1071
1967	7 Mar 1967	1430
1968	29 May 1968	2550
1969	15 Aug 1969	2590
1970	31 Jul 1970	1070
1971	27 Aug 1971	2550
1972	13 Jul 1972	1080
1973	2 Aug 1973	2380
1974	21 Dec 1973	1280
1975	15 Jul 1975	3110

Water Year	Annual Peak Flow Date	Annual Peak Flows (cfs)
1976	12 Nov 1975	868
1977	22 Mar 1977	1200
1978	8 Nov 1977	1820
1979	23 May 1979	1470
1980	28 Apr 1980	1290
1981	11 May 1981	561
1982	4 Jan 1982	1200
1983	10 Apr 1983	1330
1984	14 Dec 1983	1500
1985	27 Sep 1985	1260
1986	17 Nov 1985	1140
1987	4 Apr 1987	1110
1988	22 Jul 1988	1450
1989	20 Sep 1989	2980
1990	10 Aug 1990	1330
1991	4 Mar 1991	1340
1992	5 Jun 1992	2280
1993	1 Apr 1993	754
1994	28 Jan 1994	1430
1995	18 Jul 1995	850
1996	19 Jan 1996	1650
1999	16 Sep 1999	4800
2000	27 Jul 2000	No data
2001	30 Mar 2001	1080
2002	18 May 2002	424
2003	4 Jun 2003	1510
2004	12 May 2004	1400
2005	28 Mar 2005	1230
2006	8 Oct 2005	1050
2007	15 Apr 2007	3630
2008	6 Sep 2008	2050
2009	12 Dec 2008	1110
2010	13 Mar 2010	4080
2011	28 Aug 2011	5600
2012	08 Dec 2011	1250
2013	07 Jun 2013	2980

Water Year	Annual Peak Flow Date	Annual Peak Flows (cfs)
2014	4/30/2014	2,980
2015	1/18/2015	874
2016	2/25/2016	858
2017	6/24/2017	1,240
2018	4/16/2018	2,080
2019	7/18/2019	1,450
2020	12/14/2019	684
2021	9/1/2021	9,150
2022	10/26/2021	1,970
2023	5/1/2023	2,270

Table 20. Initial Loss and Constant Loss Rate – (Hypothetical Floods)

Subbasin	Initial Loss (in)	Constant Loss Rate (in/hr)								
		1-year	2-year	5-year	10-year	25-year	50-year	100-year	200-year	500-year
SAA	3	0.5	0.5	0.5	0.5	0.5	0.5	0.5	0.5	0.5
SAB	3	0.5	0.5	0.5	0.5	0.5	0.5	0.5	0.5	0.5
SAC	3	0.5	0.5	0.5	0.5	0.5	0.5	0.5	0.5	0.5
SAD	3	0.5	0.5	0.5	0.5	0.5	0.5	0.5	0.5	0.5
SAE	3	0.5	0.5	0.5	0.5	0.5	0.5	0.5	0.5	0.5
SAF	3	0.5	0.5	0.5	0.5	0.5	0.5	0.5	0.5	0.5
SAG	3	0.5	0.5	0.5	0.5	0.5	0.5	0.5	0.5	0.5
SAH	2.7	0.2	0.2	0.2	0.2	0.2	0.2	0.2	0.2	0.2
SAI	2.7	0.2	0.2	0.2	0.2	0.2	0.2	0.2	0.2	0.2
SAK	2.7	0.2	0.2	0.2	0.2	0.2	0.2	0.2	0.2	0.2
SAJ	2.7	0.2	0.2	0.2	0.2	0.2	0.2	0.2	0.2	0.2
SAL	3	0.2	0.2	0.2	0.2	0.2	0.2	0.2	0.2	0.2
SAM	3	0.2	0.2	0.2	0.2	0.2	0.2	0.2	0.2	0.2
RAH-N	3	0.017	0.017	0.017	0.017	0.017	0.017	0.017	0.017	0.017
102 COMP	3	0.017	0.017	0.017	0.017	0.017	0.017	0.017	0.017	0.017
101 COMP	3	0.017	0.017	0.017	0.017	0.017	0.017	0.017	0.017	0.017
ASHBRK C	3	0.017	0.017	0.017	0.017	0.017	0.017	0.017	0.017	0.017
103A COM	3	0.017	0.017	0.017	0.017	0.017	0.017	0.017	0.017	0.017
103B COM	3	0.017	0.017	0.017	0.017	0.017	0.017	0.017	0.017	0.017
103C COM	3	0.017	0.017	0.017	0.017	0.017	0.017	0.017	0.017	0.017
107 COMP	3	0.017	0.017	0.017	0.017	0.017	0.017	0.017	0.017	0.017
110 COMP	3	0.017	0.017	0.017	0.017	0.017	0.017	0.017	0.017	0.017

Table 21. The existing condition peak flows for all the HMS nodes

	1	2	5	10	25	50	100	200	500
SAA	450	517	935	1584	2476	3086	3603	4071	4747
SAA COMP	450	517	935	1584	2476	3086	3603	4071	4747
Orange_Res	206	258	445	760	1652	2476	3176	3773	4574
AB	202	253	433	731	1406	2020	2575	3083	3829
SAB	44	51	207	518	954	1250	1496	1712	2029
Junction-1	224	280	522	963	1955	2859	3677	4427	5529
LAGAB	224	280	522	963	1955	2859	3677	4427	5529
DSB	224	280	522	963	1955	2859	3677	4427	5529
Cam_Pond	224	279	522	963	1951	2855	3671	4420	5521
Dia_Mill_Pond	224	279	522	962	1951	2853	3668	4417	5519
BC	222	277	517	952	1883	2767	3537	4160	5157
Junction-2	222	277	517	952	1883	2767	3537	4160	5157
LAGBC	222	277	517	952	1883	2767	3537	4160	5157
SAC	211	239	392	604	890	1082	1239	1380	1580
WESTBR	267	318	584	1055	2051	3017	3869	4545	5663
SAD	204	244	354	505	723	888	1043	1196	1423
SAD COMP	204	244	354	505	723	888	1043	1196	1423
DE	197	237	343	487	696	856	1007	1157	1380
SAE	186	222	331	483	704	869	1023	1166	1384
DSE	365	441	639	913	1315	1623	1915	2200	2630
EF OLD R	308	373	531	747	1066	1316	1558	1802	2183
SAF	224	268	405	602	887	1101	1301	1491	1780
EASTBR	495	599	864	1231	1773	2196	2606	3016	3656
EWCONF	747	915	1447	2285	3821	5189	6425	7507	9232
CFG	670	819	1301	2033	3187	4155	4868	5867	7390
Junction-3	670	819	1301	2033	3187	4155	4868	5867	7390

	1	2	5	10	25	50	100	200	500
LAGCFG	670	819	1301	2033	3187	4155	4868	5867	7390
SAG	144	172	251	357	511	629	740	848	1010
DSG	769	939	1477	2284	3557	4629	5424	6520	8182
SAH	444	571	1113	1570	2199	2673	3124	3586	4237
DSH	1017	1275	2081	3172	4825	6393	7485	8870	10976
HI	1010	1262	2059	3123	4680	6144	7358	8778	10897
SAI	223	285	489	666	911	1101	1288	1487	1765
SPRDSI	1185	1492	2436	3634	5345	6991	8401	9988	12341
SAK	277	357	625	860	1188	1446	1698	1969	2355
DSK	1440	1829	3004	4413	6358	8247	9935	11761	14469
Lenape_Park_Dam	1191	1402	1914	2380	3260	4006	4770	5593	6911
SAJ	50	65	127	181	255	312	366	424	504
Junction-4	1213	1428	1951	2423	3317	4077	4858	5698	7045
KL1 OLD	1212	1426	1947	2415	3293	4056	4833	5686	7033
JCT KL1	1212	1426	1947	2415	3293	4056	4833	5686	7033
Junction-5	1212	1426	1947	2415	3293	4056	4833	5686	7033
KL2 OLD	1212	1426	1947	2415	3291	4051	4827	5678	7022
JCT KL2	1212	1426	1947	2415	3291	4051	4827	5678	7022
SAL	184	221	465	749	1156	1482	1806	2131	2595
DSL	1334	1564	2195	2751	3741	4639	5573	6626	8260
LM1 OLD	1334	1564	2195	2751	3741	4639	5572	6625	8259
JCT LM1	1334	1564	2195	2751	3741	4639	5572	6625	8259
Junction-6	1334	1564	2195	2751	3741	4639	5572	6625	8259
JCT LM2	1332	1562	2193	2749	3737	4633	5561	6621	8252
SAM	201	242	398	569	822	1028	1239	1454	1769
LM2 OLD	1332	1562	2193	2749	3737	4633	5561	6621	8252
RAHDSM	1501	1759	2512	3201	4254	5280	6350	7610	9529

	1	2	5	10	25	50	100	200	500
UPROBR	1497	1755	2508	3196	4250	5272	6329	7566	9477
RAH-N	49	57	105	151	216	268	319	368	431
UPROBC	1506	1773	2539	3245	4285	5312	6375	7623	9553
102 COMP	230	302	600	857	1250	1572	1907	2243	2715
101 COMP	184	258	518	743	1081	1368	1663	1973	2388
ASHBRK C	54	73	171	269	413	529	645	760	914
103A COM	11	18	47	79	125	162	199	234	281
103B COM	4	9	23	37	59	77	95	113	137
ASHIN CO	478	658	1352	1964	2899	3672	4466	5272	6374
ASHOUT R	106	180	319	442	627	790	978	1185	1540
Junction-7	106	180	319	442	627	790	978	1185	1540
104 ROUT	106	180	319	442	627	789	977	1184	1539
103C COM	17	20	38	54	77	96	115	134	160
106 COMB	108	183	324	448	635	800	991	1200	1560
107 COMP	159	188	357	511	730	912	1096	1284	1542
108 COMB	208	286	498	680	945	1168	1409	1671	2082
109 ROUT	204	286	497	678	943	1166	1408	1670	2081
110 COMP	186	232	455	660	960	1204	1453	1707	2047
111 COMB	380	506	931	1293	1826	2273	2740	3227	3905
112 ROUT	373	505	928	1288	1814	2256	2716	3197	3871
113 COMP	43	50	100	146	212	266	319	371	442
114 COMB	409	548	1014	1411	1992	2478	2983	3509	4244
115 COMP	224	264	478	671	946	1169	1399	1630	1940
116 COMB	614	791	1463	2032	2865	3555	4271	5013	6036
117 COMP	126	146	258	360	505	622	741	859	1018
118 COMB	728	917	1696	2357	3318	4114	4937	5790	6958
119 COMP	73	84	174	259	380	476	573	666	790

	1	2	5	10	25	50	100	200	500
120 COMB	792	993	1856	2588	3652	4533	5443	6381	7665
121 ROUT	681	961	1768	2452	3477	4300	5195	6117	7383
122 COMP	74	86	182	271	399	504	607	711	850
123 COMB	732	1040	1924	2676	3803	4707	5690	6702	8089
124 ROUT	730	1039	1921	2670	3796	4699	5680	6692	8079
Junction-8	730	1039	1921	2670	3796	4699	5680	6692	8079
125 ROUT	728	1037	1910	2637	3721	4605	5612	6643	8029
126 COMP	19	21	44	67	98	124	148	172	203
127 COMB	737	1052	1940	2678	3779	4678	5705	6755	8165
128 ROUT	717	1038	1834	2504	3409	4220	4928	5711	7012
129 COMP	92	105	186	262	368	454	540	626	741
130 ROBI	764	1105	1942	2645	3595	4447	5194	6019	7394
DSROBC	2178	2828	4416	5849	7773	9436	11105	12863	15950
UPSBR	2178	2827	4414	5837	7755	9427	11100	12858	15938
RAH-O	54	63	100	134	181	219	257	295	345
UPSBC	2198	2856	4457	5894	7828	9514	11188	12946	16043
201	367	462	832	1144	1595	1973	2365	2768	3342
202	346	457	806	1098	1520	1877	2252	2640	3199
203	169	216	401	557	784	973	1170	1374	1653
204	501	669	1189	1623	2251	2782	3341	3921	4748
205	481	658	1155	1570	2173	2683	3222	3787	4595
206	136	183	324	443	619	765	919	1082	1309
207	608	839	1469	1996	2763	3412	4098	4820	5850
DSSBC	2802	3695	5926	7890	10583	12913	15214	17614	21565
RTKGCR	2801	3693	5920	7874	10549	12873	15181	17580	21530
RAH-P	281	342	530	689	917	1106	1303	1510	1796
CBKGCR	3020	3973	6347	8424	11260	13730	16176	18726	22848

	1	2	5	10	25	50	100	200	500
RTARKL	3019	3971	6333	8393	11205	13637	16019	18539	22652
RAH-Q	164	217	374	506	700	860	1032	1210	1468
CBARKL	3172	4186	6693	8872	11849	14423	16937	19605	23921
Sink-1	3172	4186	6693	8872	11849	14423	16937	19605	23921

Table 22. The future condition peak flows for all the HMS nodes

	1	2	5	10	25	50	100	200	500
SAA	565	645	1115	1803	2741	3381	3921	4413	5117
SAA COMP	565	645	1115	1803	2741	3381	3921	4413	5117
Orange_Res	256	320	530	864	1942	2795	3511	4127	4940
AB	250	313	513	828	1608	2247	2824	3356	4128
SAB	44	51	207	518	954	1250	1496	1712	2029
Junction-1	273	342	610	1076	2220	3154	3996	4773	5899
LAGAB	273	342	610	1076	2220	3154	3996	4773	5899
DSB	273	342	610	1076	2220	3154	3996	4773	5899
Cam_Pond	273	341	609	1076	2215	3148	3988	4762	5888
Dia_Mill_Pond	273	341	609	1075	2214	3146	3988	4764	5889
BC	271	338	603	1062	2125	3040	3776	4444	5468
Junction-2	271	338	603	1062	2125	3040	3776	4444	5468
LAGBC	271	338	603	1062	2125	3040	3776	4444	5468
SAC	211	239	392	604	890	1082	1239	1380	1580
WESTBR	306	382	673	1170	2314	3316	4120	4857	6002
SAD	206	247	357	509	727	893	1049	1202	1429
SAD COMP	206	247	357	509	727	893	1049	1202	1429
DE	199	240	346	490	700	861	1013	1163	1387
SAE	189	225	335	488	711	877	1032	1176	1394

	1	2	5	10	25	50	100	200	500
DSE	370	446	646	922	1324	1634	1927	2213	2644
EF OLD R	312	377	537	753	1073	1324	1567	1812	2194
SAF	249	298	444	648	943	1165	1372	1569	1869
EASTBR	516	624	895	1265	1811	2238	2652	3066	3714
EWCONF	818	1002	1567	2435	4118	5521	6725	7863	9619
CFG	729	891	1403	2142	3379	4289	5052	6093	7728
Junction-3	729	891	1403	2142	3379	4289	5052	6093	7728
LAGCFG	729	891	1403	2142	3379	4289	5052	6093	7728
SAG	144	172	251	357	511	629	740	848	1010
DSG	828	1012	1581	2394	3760	4770	5615	6756	8539
SAH	476	607	1163	1630	2270	2752	3212	3682	4345
DSH	1084	1356	2200	3311	5086	6572	7695	9169	11417
HI	1074	1342	2178	3246	4891	6345	7572	9066	11307
SAI	288	360	583	775	1038	1242	1444	1656	1953
SPRDSI	1278	1609	2599	3800	5596	7251	8672	10341	12819
SAK	295	378	652	892	1226	1488	1745	2020	2412
DSK	1549	1965	3190	4598	6631	8554	10247	12162	14994
Lenape_Park_Dam	1257	1474	1976	2457	3356	4111	4886	5723	7060
SAJ	63	80	147	204	283	343	401	462	546
Junction-4	1281	1501	2013	2500	3412	4181	4970	5825	7190
KL1 OLD	1279	1499	2007	2491	3387	4159	4945	5812	7178
JCT KL1	1279	1499	2007	2491	3387	4159	4945	5812	7178
Junction-5	1279	1499	2007	2491	3387	4159	4945	5812	7178
KL2 OLD	1279	1499	2007	2491	3385	4154	4939	5804	7167
JCT KL2	1279	1499	2007	2491	3385	4154	4939	5804	7167
SAL	199	239	506	817	1261	1616	1968	2318	2816
DSL	1402	1636	2256	2819	3821	4728	5666	6741	8404

	1	2	5	10	25	50	100	200	500
LM1 OLD	1401	1636	2256	2819	3821	4728	5665	6740	8403
JCT LM1	1401	1636	2256	2819	3821	4728	5665	6740	8403
Junction-6	1401	1636	2256	2819	3821	4728	5665	6740	8403
JCT LM2	1399	1634	2252	2816	3817	4721	5654	6736	8396
SAM	208	251	412	589	851	1065	1283	1506	1832
LM2 OLD	1399	1634	2252	2816	3817	4721	5654	6736	8396
RAHDSM	1573	1838	2595	3294	4361	5401	6486	7789	9747
UPROBR	1569	1834	2591	3287	4358	5393	6464	7743	9690
RAH-N	49	57	105	151	216	268	319	368	431
UPROBC	1579	1853	2626	3341	4396	5437	6514	7804	9770
102 COMP	247	317	622	888	1290	1618	1959	2301	2780
101 COMP	194	266	531	760	1104	1396	1695	2009	2430
ASHBRK C	54	73	171	269	413	529	645	760	914
103A COM	27	31	70	110	166	211	254	294	345
103B COM	16	19	40	61	91	115	138	160	188
ASHIN CO	529	694	1410	2051	3014	3806	4619	5441	6563
ASHOUT R	113	187	327	450	636	800	989	1198	1561
Junction-7	113	187	327	450	636	800	989	1198	1561
104 ROUT	113	187	327	450	636	800	989	1198	1560
103C COM	17	20	38	54	77	96	115	134	160
106 COMB	115	190	332	457	645	811	1003	1215	1582
107 COMP	169	200	371	528	751	937	1124	1314	1576
108 COMB	221	298	515	700	970	1195	1440	1704	2112
109 ROUT	217	298	514	699	968	1194	1438	1703	2111
110 COMP	205	248	481	695	1002	1252	1508	1768	2115
111 COMB	411	534	970	1341	1888	2346	2823	3319	4010
112 ROUT	403	532	967	1335	1873	2323	2792	3281	3966

	1	2	5	10	25	50	100	200	500
113 COMP	43	50	100	146	212	266	319	371	442
114 COMB	439	576	1054	1460	2053	2548	3063	3597	4343
115 COMP	224	264	478	671	946	1169	1399	1630	1940
116 COMB	645	822	1506	2085	2930	3630	4356	5107	6143
117 COMP	150	173	290	397	549	670	793	915	1078
118 COMB	777	962	1760	2434	3412	4221	5056	5922	7106
119 COMP	73	84	174	259	380	476	573	666	790
120 COMB	842	1038	1921	2667	3748	4644	5567	6519	7822
121 ROUT	723	1006	1826	2522	3563	4395	5304	6237	7517
122 COMP	74	86	182	271	399	504	607	711	850
123 COMB	774	1085	1984	2748	3891	4803	5803	6826	8228
124 ROUT	772	1084	1980	2742	3883	4795	5792	6815	8218
Junction-8	772	1084	1980	2742	3883	4795	5792	6815	8218
125 ROUT	770	1082	1969	2706	3803	4711	5728	6763	8164
126 COMP	19	21	44	67	98	124	148	172	203
127 COMB	779	1098	1999	2747	3863	4785	5822	6877	8302
128 ROUT	758	1082	1885	2555	3475	4279	4992	5802	7109
129 COMP	92	105	186	262	368	454	540	626	741
130 ROBI	805	1151	1994	2697	3663	4506	5260	6115	7495
DSROBC	2291	2949	4569	6011	7988	9675	11368	13164	16342
UPSBR	2291	2949	4566	5999	7968	9666	11357	13162	16330
RAH-O	54	63	100	134	181	219	257	295	345
UPSBC	2312	2978	4611	6058	8043	9755	11454	13255	16441
201	378	473	848	1163	1619	1999	2396	2801	3380
202	357	468	821	1115	1541	1900	2278	2669	3232
203	172	218	404	561	788	979	1176	1381	1661
204	515	683	1207	1644	2277	2812	3374	3958	4790

	1	2	5	10	25	50	100	200	500
205	494	671	1172	1590	2196	2709	3252	3820	4633
206	143	190	335	456	634	783	939	1104	1334
207	627	859	1495	2026	2798	3451	4142	4869	5906
DSSBC	2936	3837	6106	8083	10834	13193	15546	18004	22059
RTKGCR	2935	3834	6095	8063	10797	13153	15507	17965	22020
RAH-P	281	342	530	689	917	1106	1303	1510	1796
CBKGCR	3157	4118	6524	8614	11513	14015	16511	19117	23355
RTARKL	3156	4114	6510	8586	11453	13922	16333	18915	23136
RAH-Q	164	217	374	506	700	860	1032	1210	1468
CBARKL	3310	4330	6870	9066	12100	14709	17255	19986	24414
Sink-1	3310	4330	6870	9066	12100	14709	17255	19986	24414